MAPPINGS OF FINITE DISTORTION: SIZE OF THE BRANCH SET

CHANG-YU GUO, STANISLAV HENCL, AND VILLE TENGVALL

Abstract. We study the branch set of a mapping between subsets of $\mathbb{R}^n$, i.e., the set where a given mapping is not defining a local homeomorphism. We construct several sharp examples showing that the branch set or its image can have positive measure.

1. Introduction

Let $\Omega \subset \mathbb{R}^n$, $n \geq 2$, be a domain and let us consider a continuous mapping $f : \Omega \to \mathbb{R}^n$. In many applications it is important to know when this mapping is invertible (see e.g. [5] and [30]) or at least locally invertible in many places (see e.g. [28], [12]) as the invertibility is the important key tool for the study of topological properties of the mapping. The usual proof of invertibility is to first show that the mapping is discrete (preimage $f^{-1}(y)$ of every point $y \in \mathbb{R}^n$ is a discrete set, i.e., does not have an accumulation point in Ω) and open (image of each open set is an open set), as each discrete and open mapping is invertible in many points as we mention below (see e.g. [19], [12], [20] and [16] for results in this direction). Moreover, openness and discreteness together with reasonable conditions around $\partial\Omega$ imply that the mapping is invertible.

However, every continuous, discrete and open mapping $f : \Omega \to \mathbb{R}^n$ is not necessarily injective or invertible in a neighborhood of each point in Ω. The simplest example is the winding mapping $\omega : \mathbb{R}^n \to \mathbb{R}^n$ defined as

$$\omega(x_1, x_2, x_3, \dots, x_n) = (r\cos(2\theta), r\sin(2\theta), x_3, \dots, x_n),$$

where $r = \sqrt{x_1^2 + x_2^2}$ and $\theta = \arctan(x_2/x_1)$ for $x = (x_1, x_2, \dots, x_n) \in \mathbb{R}^n$. This mapping will wind the space twice around the $(n-2)$-dimensional hyperplane $H_{n-2} := \{(0,0)\} \times \mathbb{R}^{n-2}$ and therefore it is not defining a local homeomorphism in a neighborhood of any point which lies in H_{n-2}. This kind of behavior of a mapping where the injectivity is destroyed is usually called *branching* and the set of points where a mapping f is not defining a local homeomorphism is called the *branch set* of f. We will denote the branch set and its image of a mapping f by $\mathcal{B}_f$ and $f(\mathcal{B}_f)$. These sets have very rich and complex topological and geometrical structures both of which have been studied in a variety of different context, see e.g. [1, 2, 12, 13, 14, 22, 32] and references there.

Date: June 25, 2017.
2010 *Mathematics Subject Classification.* 30C65,26B10.
Key words and phrases. Mappings of finite distortion, branch set, Lusin's condition (N).
C.Y. Guo was supported by Swiss National Science Foundation Grant 153599 and 165848. S. Hencl and V. Tengvall were supported by the ERC CZ grant LL1203 of the Czech Ministry of Education. V.T. was also supported by the Academy of Finland Project 277923.

In the case of the winding mapping we see that even if there is some branching occurring it is only happening in a very small set. Namely, the branch set $\mathcal{B}_\omega$ and its image $\omega(\mathcal{B}_\omega)$ both have topological and Hausdorff dimensions equal to $n-2$ and so have Lebesgue n-measure zero. By the theorem of Chernavskiĭ [7, 8], see also the work by Väisälä [32] for a shorter proof, for the topological dimension of these sets we have

$$\dim_{\mathcal{T}} \mathcal{B}_f = \dim_{\mathcal{T}} f(\mathcal{B}_f) \leq n-2 \tag{1.1}$$

for every continuous, discrete and open mapping f. Therefore, the size of the branch set and its image in the sense of the topological dimension are the maximal ones for the winding map. Moreover, in the case $n=2$ the branch set and its image for continuous, discrete and open mapping contains only isolated points and hence (1.1) holds in this case also for the Hausdorff dimension. However, when $n \geq 3$ there are no topological obstacles to make the branch set very large with respect to the (Lebesgue) measure and Hausdorff dimension. To see this, we simply choose a homeomorphism $g : \mathbb{R}^n \to \mathbb{R}^n$ which sends a given Cantor set of positive measure to a subset of the hyperplane H_{n-2} (see e.g. [10]) and then define

$$f := g^{-1} \circ \omega \circ g,$$

which gives us a continuous, discrete and open mapping with both sets $\mathcal{B}_f$ and $f(\mathcal{B}_f)$ having positive measure. Therefore, we need to have some additional assumptions in order to control the measure of the branch set and its image for continuous, discrete and open mappings. In this paper these additional assumptions will be given in terms of mappings of finite distortion as it is natural in many applications (see e.g. [19, 20, 16, 18, 15]):

Definition 1.1 (Mapping of finite distortion)**.** *Let $\Omega \subset \mathbb{R}^n$ be a domain with $n \geq 2$. We say that a mapping $f \in W^{1,1}_{\mathrm{loc}}(\Omega, \mathbb{R}^n)$ is a mapping of finite distortion if*

(FD-1) $J_f \in L^1_{\mathrm{loc}}(\Omega)$,

(FD-2) $J_f(x) > 0$ a.e. on the set where $|Df(x)| > 0$.

For each such a mapping we associate an outer distortion function $K_O(\cdot, f) : \Omega \to [1, \infty]$ and an inner distortion function $K_I(\cdot, f) : \Omega \to [1, \infty]$ defined as

$$K_O(x,f) = \begin{cases} \frac{|Df(x)|^n}{J_f(x)}, & \text{if } J_f(x) > 0 \\ 1, & \text{otherwise} \end{cases} \quad \text{and} \quad K_I(x,f) = \begin{cases} \frac{|D^\sharp f(x)|^n}{J_f(x)^{n-1}}, & \text{if } J_f(x) > 0 \\ 1, & \text{otherwise.} \end{cases}$$

Above, and in what follows $J_f(x) := \det Df(x)$ stands for the pointwise Jacobian and $D^\sharp f(x)$ for the pointwise adjugate matrix of the differential matrix $Df(x)$. We will refer by $|A|$ the operator norm of a matrix A. Moreover, we point out that for the distortion functions described above we have the following useful pointwise inequalities

$$K_I(x,f) \leq K_O^{n-1}(x,f) \quad \text{and} \quad K_O(x,f) \leq K_I^{n-1}(x,f)$$

for almost every $x \in \Omega$, see e.g. [18]. For the readers who are not familiar with mappings of finite distortion we recommend the monographs [4, 15, 18].

In order to study the size of the branch set and its image for mappings of finite distortion we first recall that when $K_O(\cdot, f) \in L^\infty(\Omega)$ in Definition 1.1 we recover

the well studied class of mappings of *bounded distortion*, also known as *quasiregular mappings*. Furthermore, if a mapping of bounded distortion is injective we call it *quasiconformal*. By the fundamental theorem of Reshetnyak (see e.g. [28]) every nonconstant mapping of bounded distortion is continuous, discrete and open. Moreover (see e.g. [29]), nonconstant mappings of bounded distortion

(1) are differentiable almost everywhere,
(2) have positive Jacobian almost everywhere, and
(3) satisfy Lusin's conditions (N) (i.e. every set of measure zero is mapped to a set of measure zero).

The properties listed above play an important role in the study of the size of the branch set and its image. Indeed, by [29, Lemma I.4.11] every continuous, discrete and open Sobolev mapping which is differentiable almost everywhere and has almost everywhere nonvanishing Jacobian determinant defines a local homeomorphism in a neighborhood of almost every point. In addition, if the mapping satisfies the Lusin's condition (N) then the image of the branch set will have measure zero as well. In particular, it follows that every mapping of bounded distortion has branch set and its image of zero measure. Therefore, it is natural to ask if this is the case even when the boundedness of the distortion is relaxed. The first result of this paper gives sharp conformality conditions under which continuous, discrete and open mappings of finite distortion may have branch set of positive measure. We give these conditions in terms of the inner distortion function:

Theorem 1.2. *Let $n \geq 3$ and $\Omega \subset \mathbb{R}^n$ be open. Then we have the following:*

(i) Suppose $f \in W^{1,n-1}_{\mathrm{loc}}(\Omega, \mathbb{R}^n)$ is a continuous, discrete and open mapping of finite distortion with

$$K_I(\cdot, f) \in L^1_{\mathrm{loc}}(\Omega).$$

Then f is an almost everywhere differentiable mapping with positive Jacobian determinant almost everywhere. Especially, we have $\mathcal{L}^n(\mathcal{B}_f) = 0$.

(ii) On the other hand, there exists a continuous, discrete and open Lipschitz mapping $f \in W^{1,\infty}_{\mathrm{loc}}(\mathbb{R}^n, \mathbb{R}^n)$ of finite distortion with

$$K_I(\cdot, f) \in L^p_{\mathrm{loc}}(\mathbb{R}^n)$$

for every $0 < p < 1$ such that $\mathcal{L}^n(\mathcal{B}_f) > 0$.

We should point out that the conformality and Sobolev assumptions in Theorem 1.2 are too weak to guarantee continuity, discreteness and openness of the mapping, see e.g. [16]. Because of this we will assume these conditions, in addition, to stay in the right class of mappings. The positive statement in Theorem 1.2 follows directly from the results in [22, 31]. Moreover, the local integrability assumption of the inner distortion function is sharp for the differentiability almost everywhere even in the class of $W^{1,n-1}$-homeomorphisms of finite distortion, see [17]. It is well-known that this is also the right integrability class for the inner distortion function to guarantee that the zero set of the Jacobian has null measure.

In some sense it is surprising that after we lose local integrability of the inner distortion we may find, not only $W^{1,n-1}$-mappings, but even Lipschitz mappings with the branch set of positive measure. Especially, we may see that differentiability almost everywhere is not a sufficient condition for the local invertibility almost everywhere as

every Lipschitz mapping is differentiable at almost every point. In addition, Theorem 1.2 shows the necessity of nonvanishing Jacobian almost everywhere for the local invertibility. Thus, we may ask if this is also a sufficient condition for this property. Notice that by [22] every continuous, discrete and open mapping of finite distortion with positive Jacobian almost everywhere satisfies the Lusin's condition (N^{-1}), i.e., the set $f^{-1}(E)$ has measure zero for every set $E \subset \mathbb{R}^n$ of measure zero. Therefore, to construct a continuous, discrete and open mapping of finite distortion with a positive Jacobian almost everywhere and with the branch set of positive measure it is necessary to have the measure of the image of the branch positive as well. In the main result of this paper we will construct such a mapping showing that the condition $J_f > 0$ is not sufficient for the local invertibility:

Theorem 1.3. *Let $n = 3$. There exists a continuous, discrete and open mapping of finite distortion such that $f \in W^{1,p}((-1,1)^3, (-1,1)^3)$ for all $p \in [1,2)$, $J_f > 0$ almost everywhere, but*

$$\mathcal{L}^n(\mathcal{B}_f) > 0 \quad \textit{and} \quad \mathcal{L}^n(f(\mathcal{B}_f)) > 0.$$

Recall that by the differentiability result of Väisälä [34] every continuous and open mapping in $W^{1,p}$, $p > n-1$, is differentiable almost everywhere, and on the other hand differentiability might fail for mappings in $W^{1,n-1}$ even if they are assumed to be homeomorphisms of finite distortion with positive Jacobian almost everywhere, see e.g. [9]. Hence, it would be interesting to know what happens for the size of the branch set in Theorem 1.3 in the borderline case where $f \in W^{1,n-1}$ as it could also tell if the differentiability almost everywhere is a necessary condition for the local invertibility. It is possible to slightly improve the Sobolev regularity of the mapping in Theorem 1.3 on logarithmic scale, and to derive some level of integrability for the distortion functions of this mapping, see section 7. However, we do not know what are the sharp Lorentz conditions and distortion assumptions under which a continuous, discrete and open mapping of finite distortion with positive Jacobian almost everywhere will have branch set of zero measure. For the sharp Lorentz condition for the differentiability without any additional conformality conditions we refer to [26].

There are several reasons to study the branch set of mappings of finite distortion. One such a reason can be seen when we try to generalize the well-known Poletsky's [27] and Väisälä's [33] moduli inequalities of quasiregular mappings, or the corresponding capacity inequalities, see e.g. [24, 25, 32], for mappings of finite distortion. These inequalities were generalized for mappings of finite distortion in $W^{1,n}_{\mathrm{loc}}$ with locally integrable inner distortion by Koskela and Onninen [23]. The optimal assumptions for these inequalities with lower regularity assumptions were further studied in [11, 17, 31]. As it was observed in [11], these inequalities would follow for a continuous, discrete and open mapping f of finite distortion with even lower regularity assumptions by following the standard arguments in the theory of quasiregular mappings whenever

(1) the mapping f is differentiable almost everywhere,
(2) the Jacobian determinant is positive almost everywhere,
(3) the branch set $\mathcal{B}_f$ has measure zero, and
(4) the image $f(\mathcal{B}_f)$ has measure zero as well.

It follows from [22, 31] that the conditions (1)–(3) hold whenever we have a continuous, discrete and open mapping $f \in W^{1,n-1}_{\mathrm{loc}}(\Omega, \mathbb{R}^n)$ of finite distortion with locally integrable inner distortion. However, we need to have much stronger assumptions if we want (4) to hold:

Theorem 1.4. *Let $\Omega \subset \mathbb{R}^n$ be an open set with $n \geq 3$. Then we have the following:*

(i) If $f : \Omega \to \mathbb{R}^n$ is a nonconstant mapping of finite distortion with

$$\exp\big(K_O(\cdot, f)\big) \in L^1_{\mathrm{loc}}(\Omega),$$

then f is continuous, discrete and open. Moreover, f satisfies Lusin's condition (N) and $\mathcal{L}^n(f(\mathcal{B}_f)) = 0$.

(ii) On the other hand, for each $0 < \varepsilon < 1$ there is a continuous, discrete and open mapping $f \in W^{1,p}_{\mathrm{loc}}(\mathbb{R}^n, \mathbb{R}^n)$, for all $1 \leq p < n$, of finite distortion such that

$$\exp\Big(K_O^{1-\varepsilon}(\cdot, f)\Big) \in L^1_{\mathrm{loc}}(\mathbb{R}^n)$$

and $\mathcal{L}^n(f(\mathcal{B}_f)) > 0$.

Theorem 1.4 shows the necessity of Lusin's condition (N) for the condition $\mathcal{L}^n(f(\mathcal{B}_f)) = 0$. We will see in section 3 that Theorem 1.4 (ii) follows from an even stronger result, Theorem 3.2. The positive statement in Theorem 1.4 is originally proved in [21].

2. Preliminaries

2.1. **Notation.** A point $x \in \mathbb{R}^n$ in coordinates is denoted as $(x_1, x_2, \ldots, x_n)$ and its *Euclidean* and *supremum norms* are denoted by $|x| := \sqrt{\sum_{i=1}^n x_i^2}$ and $\|x\| := \sup_i |x_i|$. Furthermore, we will denote by

$$Q(a, r) := (a_1 - r, a_1 + r) \times \cdots \times (a_n - r, a_n + r)$$

an open cube centered at $a \in \mathbb{R}^n$ with side-length $2r > 0$. The interior of a set $A \subset \mathbb{R}^n$ is denoted by A° and the symbol $\mathcal{L}^n$ refers to the Lebesgue n-measure. When write

$$C := C(p_1, \ldots, p_k)$$

we mean a positive constant which depends only on the given parameters $p_1, \ldots p_k$. The constant C might change from line to line. Furthermore, for given functions f and g we denote $f \lesssim g$ if there exists a positive constant $C > 0$ such that $f(x) \leq Cg(x)$ for all points x. In the case when both conditions $f \lesssim g$ and $g \lesssim f$ are satisfied we denote $f \sim g$.

2.2. **Sobolev spaces.** Let $\Omega \subset \mathbb{R}^n$ be an open set. The *Sobolev space* $W^{1,p}(\Omega, \mathbb{R}^m)$, $1 \leq p \leq \infty$, will consist all the mappings

$$f := (f_1, \ldots, f_m) : \Omega \to \mathbb{R}^m$$

such that for the real-valued coordinate functions and for their distributional partial derivatives we have

$$f_i \in L^p(\Omega) \quad \text{and} \quad \frac{\partial f_i}{\partial x_j} \in L^p(\Omega)$$

for all $i = 1, \ldots, m$ and for every $j = 1, \ldots, n$. If $f \in W^{1,p}(\Omega', \mathbb{R}^m)$ for every subdomain $\Omega' \subset\subset \Omega$ we denote $f \in W^{1,p}_{\mathrm{loc}}(\Omega, \mathbb{R}^m)$.

2.3. **ACL condition.** Let $i \in \{1, 2, \dots, n\}$ and denote by π_i the projection on the given hyperplane $H_i = \{x \in \mathbb{R}^m : x_i = 0\}$ perpendicular to the x_i-axis. We say that a mapping $f \in L^1_{\mathrm{loc}}(\Omega, \mathbb{R}^m)$ is *absolutely continuous* (on lines) if the following ACL condition holds:

(ACL) For every cube $Q(a, r) = (a_1 - r, a_1 + r) \times \cdots \times (a_n - r, a_n + r) \subset\subset \Omega$ and for every $i \in \{1, 2, \dots, n\}$ the coordinate functions

$$f^i(t; x) := f(x_1, \dots, x_{i-1}, x_i + t, x_{i+1}, \dots, x_n)$$

are absolutely continuous on $(a_i - r, a_i + r)$ for $\mathcal{L}^{n-1}$-almost every $x \in \pi_i(Q(a, r))$.

The following characterization of Sobolev spaces is classical and can be found e.g. in [3, Section 3.11] and [15, Theorem A.15]:

Proposition 2.1. *Let $1 \le p < \infty$, $\Omega \subset \mathbb{R}^n$ be an open set and $f \in L^p(\Omega, \mathbb{R}^m)$. Then $f \in W^{1,p}_{\mathrm{loc}}(\Omega, \mathbb{R}^n)$ if and only if there is a representative of f which is a $\mathrm{ACL}(\Omega, \mathbb{R}^m)$ mapping with locally L^p-integrable partial derivatives on Ω.*

2.4. **Conditions (N) and (N^{-1}), and the area formula.** Suppose $f : \Omega \to \mathbb{R}^n$ is a mapping defined on an open set $\Omega \subset \mathbb{R}^n$ with $n \ge 1$.

(1) We say that f satisfies *Lusin's condition* (N) if for each set $E \subset \Omega$ such that $\mathcal{L}^n(E) = 0$ we have $\mathcal{L}^n(f(E)) = 0$.

(2) We say that f satisfies *Lusin's condition* (N^{-1}) if for each set $F \subset \mathbb{R}^n$ such that $\mathcal{L}^n(F) = 0$ we have $\mathcal{L}^n(f^{-1}(F)) = 0$.

We will need the following well-known area formula for Sobolev mappings (see e.g. [15, Theorem A.12]):

Proposition 2.2. *Let $f \in W^{1,1}_{\mathrm{loc}}(\Omega, \mathbb{R}^n)$ and let η be a nonnegative Borel measurable function on $\mathbb{R}^n$. Then*

$$\int_\Omega \eta(f(x)) |J(x, f)| \, \mathrm{d}x \le \int_{\mathbb{R}^n} \eta(y) N(y, f, \Omega) \, \mathrm{d}y, \tag{2.1}$$

where the multiplicity function $N(y, f, \Omega)$ is defined as the number of points in the set $f^{-1}(y) \cap \Omega$ for $y \in \mathbb{R}^n$. Moreover, there is an equality in (2.1) if we assume in addition that f satisfies the Lusin's condition (N).

2.5. **Constructing Cantor sets.** Suppose $[-1, 1]^n \subset \mathbb{R}^n$, and denote by $\mathbb{V}$ the set of 2^n vertices of the cube $[-1, 1]^n$. The sets

$$\mathbb{V}^k = \mathbb{V} \times \cdots \times \mathbb{V}, \quad k \in \mathbb{N},$$

will serve as the set of indices for our construction.

Next, suppose $\{a_k\}_{k=0}^\infty$ is a decreasing sequence such that $1 = a_0 \ge a_1 \ge \cdots > 0$, and define

$$r_k = 2^{-k} a_k \, .$$

Set $z_0 = 0$. Then it follows that $Q(z_0, r_0) = (-1, 1)^n$ and we proceed further by induction. For $\boldsymbol{v}(k) = (v_1, \dots, v_k) \in \mathbb{V}^k$ we denote $\boldsymbol{w}(k) = (v_1, \dots, v_{k-1})$ and define

(see Fig. 1)

$$z_{\boldsymbol{v}(k)} = z_{\boldsymbol{w}(k)} + \frac{1}{2} r_{k-1} v_k = z_0 + \frac{1}{2} \sum_{j=1}^{k} r_{j-1} v_j,$$

$$Q'_{\boldsymbol{v}(k)} = Q(z_{\boldsymbol{v}(k)}, 2^{-k} a_{k-1}) \text{ and } Q_{\boldsymbol{v}(k)} = Q(z_{\boldsymbol{v}(k)}, 2^{-k} a_k)\,.$$

Then for the measure of the k-th frame $Q'_{\boldsymbol{v}(k)} \backslash Q_{\boldsymbol{v}(k)}$ we have

$$\mathcal{L}^n(Q'_{\boldsymbol{v}(k)} \backslash Q_{\boldsymbol{v}(k)}) = 2^{-kn}(a_{k-1}^n - a_k^n)\,. \tag{2.2}$$

Formally we should write $\boldsymbol{w}(\boldsymbol{v}(k))$ instead of $\boldsymbol{w}(k)$ but for the simplification of the notation we will avoid this.

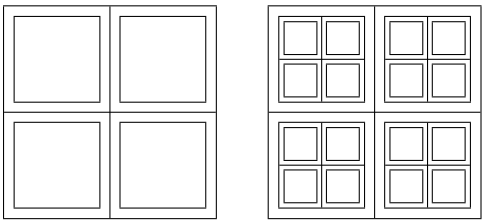

Fig. 1 Cubes $Q_{\boldsymbol{v}(k)}$ and $Q'_{\boldsymbol{v}(k)}$ for $k = 1, 2$.

It is not difficult to find out that the resulting Cantor set

$$\bigcap_{k=1}^{\infty} \bigcup_{\boldsymbol{v}(k) \in \mathbb{V}^k} Q_{\boldsymbol{v}(k)} =: C[\{a_k\}_{k=0}^{\infty}] = \mathcal{C}_a \times \cdots \times \mathcal{C}_a$$

is a product of n Cantor sets $\mathcal{C}_a$ in $\mathbb{R}$, and the number of the cubes $\{Q_{\boldsymbol{v}(k)} : \boldsymbol{v}(k) \in \mathbb{V}^k\}$ is 2^{nk}. Therefore, the measure of the Cantor set $C_A := C[\{a_k\}_k]$ can be calculated as

$$\mathcal{L}^n(C_A) = \lim_{k \to \infty} 2^{nk} (2 a_k 2^{-k})^n = \lim_{k \to \infty} 2^n a_k^n\,. \tag{2.3}$$

2.6. **Homeomorphism that maps a Cantor set onto another one.** Let us first recall [15, Lemma 2.1].

Lemma 2.3. *Let $\rho : (0, \infty) \to (0, \infty)$ be a strictly monotone function and $\rho \in C^1((0, \infty))$. Then for the mapping*

$$f(x) = \frac{x}{\|x\|} \rho(\|x\|), \quad x \neq 0$$

we have for almost every x

$$|Df(x)| \sim \max\Big\{ \frac{\rho(\|x\|)}{\|x\|}, |\rho'(\|x\|)| \Big\} \text{ and } J_f(x) \sim \rho'(\|x\|) \Big(\frac{\rho(\|x\|)}{\|x\|} \Big)^{n-1}\,.$$

In fact, this lemma is shown in [15] for the Euclidean norm $|x|$ but by a bi-Lipschitz change of variables it it easy to see that the same formula holds also for the supremum norm $\|x\| = \max_{i=1,\dots,n} |x_i|$ analogously to [15, Chapter 4.3].

Suppose

$$C_A := C[\{a_k\}_{k=0}^{\infty}] \quad \text{and} \quad C_B := C[\{b_k\}_{k=0}^{\infty}]$$

are two Cantor sets which we get by applying the algorithm in section 2.5 to the sequences $\{a_k\}_{k=0}^{\infty}$ and $\{b_k\}_{k=0}^{\infty}$. Following section 2.5 we define

$$r_k = 2^{-k}a_k, \quad r'_k = 2^{-k}a_{k-1}, \quad \tilde{r}_k = 2^{-k}b_k, \quad \tilde{r}'_k = 2^{-k}b_{k-1},$$
$$z_{\boldsymbol{v}(k)} = z_{\boldsymbol{w}(k)} + \frac{1}{2}r_{k-1}v_k = z_0 + \frac{1}{2}\sum_{j=1}^{k} r_{j-1}v_j \quad \text{and}$$
$$\tilde{z}_{\boldsymbol{v}(k)} = \tilde{z}_{\boldsymbol{w}(k)} + \frac{1}{2}\tilde{r}_{k-1}v_k = \tilde{z}_0 + \frac{1}{2}\sum_{j=1}^{k} \tilde{r}_{j-1}v_j.$$

Furthermore, we also define

$$Q'_{\boldsymbol{v}(k)} = Q(z_{\boldsymbol{v}(k)}, r'_k), \quad Q_{\boldsymbol{v}(k)} = Q(z_{\boldsymbol{v}(k)}, r_k)$$
$$\tilde{Q}'_{\boldsymbol{v}(k)} = Q(\tilde{z}_{\boldsymbol{v}(k)}, \tilde{r}'_k), \quad \tilde{Q}_{\boldsymbol{v}(k)} = Q(\tilde{z}_{\boldsymbol{v}(k)}, \tilde{r}_k).$$

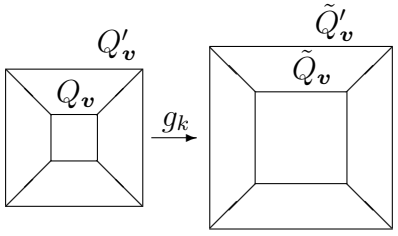

Fig. 2 The transformation of $Q'_{\boldsymbol{v}} \setminus Q^{\circ}_{\boldsymbol{v}}$ onto $\tilde{Q}'_{\boldsymbol{v}} \setminus \tilde{Q}^{\circ}_{\boldsymbol{v}}$

It remains to find a homeomorphism g which maps C_A onto C_B. We will find a sequence of homeomorphisms $g_k : (-1,1)^n \to (-1,1)^n$. Set $g_0(x) = x$ and we proceed by induction. We will give a mapping g_1 which stretches each cube $Q_{\boldsymbol{v}}$, $\boldsymbol{v} \in \mathbb{V}^1$, homogeneously so that $g_1(Q_{\boldsymbol{v}})$ equals $\tilde{Q}_{\boldsymbol{v}}$. On the annulus $Q'_{\boldsymbol{v}} \setminus Q_{\boldsymbol{v}}$, g_1 is defined to be an appropriate radial map with respect to $z_{\boldsymbol{v}}$ and $\tilde{z}_{\boldsymbol{v}}$ in the image in order to make g_1 a homeomorphism. The general step is the following: If $k > 1$, g_k is defined as g_{k-1} outside the union of all cubes $Q_{\boldsymbol{w}}$, $\boldsymbol{w} \in \mathbb{V}^{k-1}$. Further, g_k remains equal to g_{k-1} at the centers of cubes $Q_{\boldsymbol{v}}$, $\boldsymbol{v} \in \mathbb{V}^k$. Then g_k stretches each cube $Q_{\boldsymbol{v}}$, $\boldsymbol{v} \in \mathbb{V}^k$, homogeneously so that $g_k(Q_{\boldsymbol{v}})$ equals $\tilde{Q}_{\boldsymbol{v}}$. On the annulus $Q'_{\boldsymbol{v}} \setminus Q_{\boldsymbol{v}}$, g_k is defined to be an appropriate radial map with respect to $z_{\boldsymbol{v}}$ in preimage and $\tilde{z}_{\boldsymbol{v}}$ in image to make g_k a homeomorphism (see Fig. 2). Notice that the Jacobian determinant $J_{g_k}(x)$ will be strictly positive almost everywhere in $(-1,1)^n$.

In this construction we use the notation $\|x\|$ for the supremum norm of $x \in \mathbb{R}^n$. The mappings g_k, $k \in \mathbb{N}$, are formally defined as

$$g_k(x) = \begin{cases} g_{k-1}(x) & \text{for } x \notin \bigcup_{\boldsymbol{v}\in\mathbb{V}^k} Q'_{\boldsymbol{v}} \\ g_{k-1}(z_{\boldsymbol{v}}) + (\alpha_k\|x - z_{\boldsymbol{v}}\| + \beta_k)\frac{x-z_{\boldsymbol{v}}}{\|x-z_{\boldsymbol{v}}\|} & \text{for } x \in Q'_{\boldsymbol{v}} \setminus Q_{\boldsymbol{v}},\ \boldsymbol{v} \in \mathbb{V}^k \\ g_{k-1}(z_{\boldsymbol{v}}) + \frac{\tilde{r}_k}{r_k}(x - z_{\boldsymbol{v}}) & \text{for } x \in Q_{\boldsymbol{v}},\ \boldsymbol{v} \in \mathbb{V}^k \end{cases} \tag{2.4}$$

where the constants α_k and β_k are given by

$$\alpha_k r_k + \beta_k = \tilde{r}_k \text{ and } \alpha_k \tfrac{r_{k-1}}{2} + \beta_k = \tfrac{\tilde{r}_{k-1}}{2}. \tag{2.5}$$

It is not difficult to find out that each g_k is a homeomorphism and maps

$$\bigcup_{\boldsymbol{v}\in\mathbb{V}^k} Q_{\boldsymbol{v}} \text{ onto } \bigcup_{\boldsymbol{v}\in\mathbb{V}^k} \tilde{Q}_{\boldsymbol{v}}.$$

The mapping $g(x) = \lim_{k\to\infty} g_k(x)$ is clearly one to one and continuous and therefore it is a homeomorphism. Moreover, it is not difficult to see that g is differentiable almost everywhere, absolutely continuous on almost all lines parallel to coordinate axes and maps C_A onto C_B (see [15, Chapter 4.3] for details).

Let $k \in \mathbb{N}$ and $\boldsymbol{v} \in \mathbb{V}^k$. We need to estimate $Dg(x)$ in the interior of the annulus $Q'_{\boldsymbol{v}} \setminus Q_{\boldsymbol{v}}$. Since

$$g(x) = g(z_{\boldsymbol{v}}) + (\alpha_k\|x - z_{\boldsymbol{v}}\| + \beta_k)\frac{x - z_{\boldsymbol{v}}}{\|x - z_{\boldsymbol{v}}\|}$$

we obtain from Lemma 2.3 and (2.5) that

$$Dg(x) \sim \max\Big\{\frac{\tilde{r}_k}{r_k}, \alpha_k\Big\} = \max\Big\{\frac{\tilde{r}_k}{r_k}, \frac{\frac{\tilde{r}_{k-1}}{2} - \tilde{r}_k}{\frac{r_{k-1}}{2} - r_k}\Big\}. \tag{2.6}$$

and

$$J_g(x) \sim \alpha_k\Big(\frac{\tilde{r}_k}{r_k}\Big)^{n-1} = \frac{\frac{\tilde{r}_{k-1}}{2} - \tilde{r}_k}{\frac{r_{k-1}}{2} - r_k}\Big(\frac{\tilde{r}_k}{r_k}\Big)^{n-1}. \tag{2.7}$$

2.7. **Constructing Cantor's tower.** Suppose $n \geq 2$ and denote by $\hat{\mathbb{V}}$ the set of points

$$\big(0, 0, \ldots, 0, -1 + \tfrac{2j}{2^n}\big)$$

where $j = 1, 2, \ldots, 2^n$. The sets

$$\hat{\mathbb{V}}^k := \hat{\mathbb{V}} \times \cdots \times \hat{\mathbb{V}}, \quad k \in \mathbb{N},$$

will serve as the set of indices in the construction of Cantor's tower.

Suppose next $\{c_k\}_{k=0}^{\infty}$ is a decreasing sequence such that $1 = c_0 \geq c_1 \geq c_2 \geq \cdots > 0$, and define

$$\hat{r}_k := 2^{-nk}c_k.$$

Set $\hat{z}_0 = 0$. Then it follows that $Q(\hat{z}_0, \hat{r}_0) = (-1, 1)^n$ and we proceed further by induction. For $\hat{\boldsymbol{v}}(k) := (\hat{v}_1, \hat{v}_2, \ldots, \hat{v}_k) \in \hat{\mathbb{V}}^k$ we denote $\hat{\boldsymbol{w}}(k) := (\hat{v}_1, \hat{v}_2, \ldots, \hat{v}_{k-1})$ and define (see Fig. 3)

$$\hat{z}_{\boldsymbol{v}(k)} := \hat{z}_{\hat{\boldsymbol{w}}(k)} + \hat{r}_{k-1}\hat{v}_k = \hat{z}_0 + \sum_{j=1}^{k} \hat{r}_{j-1}\hat{v}_j$$

$$\hat{Q}'_{\boldsymbol{v}(k)} := Q(\hat{z}_{\hat{\boldsymbol{v}}(k)}, 2^{-nk}c_{k-1}) \text{ and } \hat{Q}_{\boldsymbol{v}(k)} := Q(\hat{z}_{\hat{\boldsymbol{v}}(k)}, 2^{-nk}c_k)$$

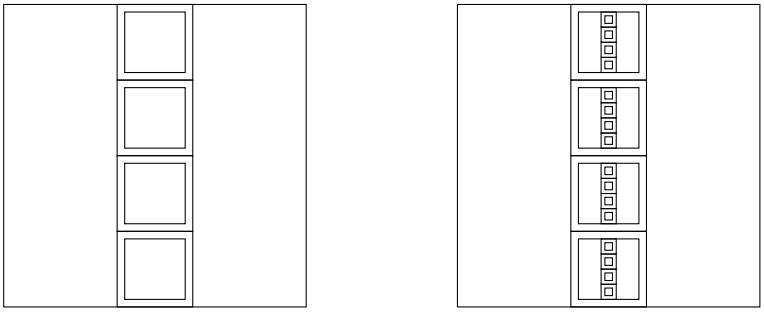

Fig. 3 Cubes $\hat{Q}_{\boldsymbol{v}(k)}$ and $\hat{Q}'_{\boldsymbol{v}(k)}$ for $k = 1, 2$ in the construction of the Cantor's tower.

2.8. **Bi-Lipschitz mapping which takes a Cantor set onto a Cantor's tower.** Let us now define the Cantor set C_B in section 2.5 by choosing

$$b_k = 2^{-k\beta},$$

where $\beta \geq n+1$. Similarly, we define the Cantor's tower C_C^T in section 2.7 by choosing

$$c_k = 2^{-k\beta}.$$

As $\beta \geq n+1$, we see that

$$\hat{Q}'_{\boldsymbol{v}(k)} = Q(\hat{z}_{\hat{\boldsymbol{v}}(k)}, 2^{-k}c_k) \subset Q(\hat{z}_{\hat{\boldsymbol{v}}(k)}, 2^{-1-nk}c_{k-1}) = \frac{1}{2}\hat{Q}'_{\boldsymbol{v}(k)} \tag{2.8}$$

and thus we have enough empty space in $\hat{Q}'_{\boldsymbol{v}(k)} \setminus \hat{Q}'_{\boldsymbol{v}(k)}$ to move the cubes of the next generation into a tower formation.

The following proposition will give us a bi-Lipschitz mapping $F : \mathbb{R}^n \to \mathbb{R}^n$ which maps the Cantor set C_B onto Cantor's tower C_B^T. We will refer to this mapping as a *tower mapping* and it is applied to prove theorems 1.2 and 1.4. Later we need to refine this mapping further in order to prove Theorem 1.3.

Proposition 2.4. *Suppose that C_B is the Cantor set and C_B^T the Cantor's tower in $\mathbb{R}^n$ defined by the sequence*

$$b_k = 2^{-k\beta},$$

where $\beta \geq n+1$. Then there is a bi-Lipschitz mapping $L : \mathbb{R}^n \to \mathbb{R}^n$ which takes C_B onto C_B^T.

Proof. We construct bi-Lipschitz mappings L_j which take the j-th step of the construction of C_B onto the j-th step of the construction of C_B^T. All L_j are bi-Lipschitz with the same constant and the limit $F = \lim_{j\to\infty} L_j$ is thus bi-Lipschitz as well.

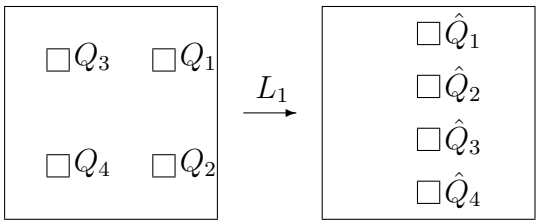

Fig. 4 Construction of L_1 which translates Q_i onto $\hat{Q}_i$.

We claim that there is a bi-Lipschitz mapping $L_1 : [-1,1]^n \to [-1,1]^n$ such that (see Fig. 4)

$$L_1(x) = x \text{ for every } x \in \partial[-1,1]^n \text{ and}$$
$$L_1(x) = x - z_{\boldsymbol{v}(1)} + \hat{z}_{\boldsymbol{v}(1)} \text{ for every } x \in Q_{\boldsymbol{v}(1)}.$$

This means that L_1 fixes the boundary and it is a just a translation of each of the 2^n cubes $Q_{\boldsymbol{v}(1)}$ onto $\hat{Q}_{\boldsymbol{v}(1)}$. As $\beta \geq n+1$ we have enough space for doing this (see (2.8)) and it is not difficult to see that such a homeomorphism exists (see Fig. 4) and it can be constructed as a bi-Lipschitz mapping. Formally we should give the exact formula for the mapping which would not be difficult but it would be extremely lengthy. We skip this as the construction of such F_1 is trustworthy and not difficult to see from the picture. More details and the construction of admissible F_1 for $n = 3$ can be found in Section 7. In fact the construction there is slightly different as we map cubes $Q_{\boldsymbol{v}(1)}$ onto $\hat{Q}_{\boldsymbol{v}(1)}$ but the mapping is not necessarily just a translation there.

We continue by constructing L_2 as a scaled copy of L_1 into each $Q_{\boldsymbol{v}(1)}$. Formally, we set

$$L_2(x) = \begin{cases} L_1(x) & \text{for } x \in [-1,1]^n \setminus \bigcup_{\boldsymbol{v}(1)\in\mathbb{V}^1} Q_{\boldsymbol{v}(1)}, \\ \hat{z}_{\boldsymbol{v}(1)} + 2^{-1-\beta} L_1\big(2^{1+\beta}(x - z_{\boldsymbol{v}(1)})\big) & \text{for } x \in Q_{\boldsymbol{v}(1)}. \end{cases}$$

As the constructions of C_B and C_B^T are self-similar it is not difficult to see that F_2 translates each $Q_{\boldsymbol{v}(2)}$ onto the corresponding $\hat{Q}_{\boldsymbol{v}(2)}$. We claim that L_2 has the same bi-Lipschitz constant $L > 0$ as L_1. For $x, y \in Q_{\boldsymbol{v}(1)}$ we can estimate

$$\begin{aligned} |L_2(x) - L_2(y)| &\leq 2^{-1-\beta} \big| L_1\big(2^{1+\beta}(x - z_{\boldsymbol{v}(1)}) - L_1\big(2^{1+\beta}(y - z_{\boldsymbol{v}(1)})\big| \\ &\leq 2^{-1-\beta} L 2^{1+\beta} |x - y| = L|x - y| \ . \end{aligned}$$

and a similar estimate holds from below. If $x \in Q_{\boldsymbol{v}(1)}$ and $y \notin Q_{\boldsymbol{v}(1)}$ we can connect x and y by a segment, divide this segment by points on the boundaries of $\bigcup_{\boldsymbol{v}(1)\in\mathbb{V}^1} Q_{\boldsymbol{v}(1)}$, use the estimate on each part of the segment separately and sum up. Thus F_2 is also L-bi-Lipschitz.

We continue by induction and we set

$$L_{k+1}(x) = \begin{cases} L_k(x) & \text{for } x \in [-1,1]^n \setminus \bigcup_{\boldsymbol{v}(k)\in\mathbb{V}^k} Q_{\boldsymbol{v}(k)}, \\ \hat{z}_{\boldsymbol{v}(k)} + 2^{(-1-\beta)k} L_1\big(2^{k(1+\beta)}(x - z_{\boldsymbol{v}(k)})\big) & \text{for } x \in Q_{\boldsymbol{v}(k)}. \end{cases}$$

Similarly as for L_2 we obtain that L_{k+1} is L-bi-Lipschitz and it maps each $Q_{\boldsymbol{v}(k+1)}$ onto the corresponding $\hat{Q}_{\boldsymbol{v}(k+1)}$ affinely. The limiting map $F(x) = \lim_{j\to\infty} L_j(x)$ is thus L-bi-Lipschitz and maps C_B onto C_B^T. □

3. Proof of Theorem 1.4: the size of $f(\mathcal{B}_f)$

We have already noticed in the introduction that if f has "reasonably nice" properties then the set $f(\mathcal{B}_f)$ has measure zero. The next lemma specifies these reasonably nice properties.

Lemma 3.1. *Suppose f is a continuous, sense-preserving, discrete and open mapping which is differentiable almost everywhere and satisfies Lusin's condition (N). Then $\mathcal{L}^n(f(\mathcal{B}_f)) = 0$.*

Proof. Since the issue is local, we may assume that f has bounded multiplicity [29, Proposition I.4.10 (3)]. Let us denote

$$A := \{x \in \mathcal{B}_f : f \text{ is not differentiable at } x\} \text{ and}$$
$$B := \{x \in \mathcal{B}_f : f \text{ is differentiable at } x\}.$$

Then we may write $\mathcal{B}_f = A \cup B$. Because f is differentiable almost everywhere we have $\mathcal{L}^n(A) = 0$ and hence it follows from Lusin's condition (N) that

$$\mathcal{L}^n(f(A)) = 0. \tag{3.1}$$

On the other hand, by [29, Lemma I.4.11] we have $J_f(x) = 0$ for every $x \in B$, and thus the area formula (see Proposition 2.2) implies

$$\int_{f(B)} N(y, f, f(B))\,\mathrm{d}x = \int_B |J_f|(x)\,\mathrm{d}x = 0. \tag{3.2}$$

As $N(y, f, f(B)) \geq 1$ on $f(B)$ we obtain that $\mathcal{L}^n(f(B)) = 0$ and it follows from (3.1) that

$$\mathcal{L}^n(f(\mathcal{B}_f)) \leq \mathcal{L}^n(f(A)) + \mathcal{L}^n(f(B)) = 0.$$

□

The following theorem stresses out the importance of the Lusin's condition (N). Namely, without the condition (N) we cannot assure that the set $f(\mathcal{B}_f)$ has measure zero even when the branch set $\mathcal{B}_f$ has measure zero.

Theorem 3.2. *There exists a discrete and open mapping $f : \mathbb{R}^n \to \mathbb{R}^n$, $n \geq 3$, with the following properties:*

1) *$f \in W^{1,p}_{\mathrm{loc}}(\mathbb{R}^n, \mathbb{R}^n)$ for all $1 \leq p < n$,*
2) *f is a mapping of finite distortion, and the outer distortion $K_O(\cdot, f)$ satisfies*
$$\exp\big(\Psi(K_O(x, f))\big) \in L^1_{\mathrm{loc}}(\mathbb{R}^n),$$
where $\Psi : (0, \infty) \to (0, \infty)$ is a strictly increasing, concave, continuous function such that
$$\int_1^\infty \frac{\Psi'(t)}{t}\,\mathrm{d}t < \infty,$$
3) *the inner distortion $K_I(\cdot, f)$ satisfies*
$$\exp\big(\Psi^*(K_I(x, f))\big) \in L^1_{\mathrm{loc}}(\mathbb{R}^n),$$
where $\Psi^*(t) = \Psi\big(t^{1/(n-1)}\big)$,
4) *the mapping f is differentiable almost everywhere, the Jacobian of f is strictly positive almost everywhere and f satisfies Lusin's condition (N^{-1}), and*
5) *$\mathcal{L}^n\big(\mathcal{B}_f\big) = 0$, but $\mathcal{L}^n\big(f(\mathcal{B}_f)\big) > 0$.*

Proof. Suppose that $\omega : \mathbb{R}^n \to \mathbb{R}^n$ is the winding mapping defined as in the introduction. Then ω is a quasiregular mapping with the branch set $\mathcal{B}_\omega = \{(0, 0)\} \times \mathbb{R}^{n-2}$.

Let us define Cantor sets $C_A := C[\{a_k\}_{k=0}^\infty]$ and $C_B := C[\{b_k\}_{k=0}^\infty]$ (see section 2.5) by setting

$$a_k := \frac{1}{2}\big(1 + 2^{-2k}\big) \quad \text{and} \quad b_k = 2^{-2k}.$$

Then it follows that

$$\mathcal{L}^n(C_A) > 1 \quad \text{and} \quad \mathcal{L}^n(C_B) = 0.$$

Let $g : \mathbb{R}^n \to \mathbb{R}^n$ be a quasiconformal mapping such that $C_B \subset g(\{0\}^{n-1} \times [-1,1])$, where $\{0\}^{n-1}$ stands for the origin in $\mathbb{R}^{n-1}$. For the existence of such a mapping see e.g. [6, Lemma 3.1] or apply the tower mapping from section 2.8. Because a composition of two quasiregular mapping is also quasiregular we find out that

$$h := g \circ \omega$$

defines a quasiregular mapping. Especially, there exists a finite constant $K_h \geq 1$ such that

$$|Dh(x)|^n \leq K_h J_h(x) \quad \text{a.e.}$$

Suppose next Ψ and Ψ^* are defined as in the theorem. Then by [21] there exists a homeomorphism $F : [-1,1]^n \to [-1,1]^n$ that fixes the boundary $\partial Q(0,1)$ and has the following properties:

(a) $F \in W^{1,1}((-1,1)^n, \mathbb{R}^n)$, F is differentiable almost everywhere, and

$$F \in W^{1,q}((-1,1)^n, \mathbb{R}^n) \text{ for every } 1 \leq q < n.$$

This follows from $|DF(x)^n \leq K_O(x,F) J_F(x)$, $J_F \in L^1$ and $K_O(x,F) \in L^a$ for every $a < \infty$.

(b) The Jacobian determinant $J_F(x)$ is positive almost everywhere, and

$$\int_{(-1,1)^n} J_F(x)\,\mathrm{d}x < \infty\,.$$

(c) The distortion $K_O(x,F)$ is finite almost everywhere, and for every $\lambda > 0$

$$\int_{(-1,1)^n} \exp\big(\lambda\, \Psi(K_O(x,F))\big)\,\mathrm{d}x < \infty\,,$$

where Ψ is given as in the statement (2) of the Theorem 3.2.

(d) The mapping F maps a Cantor set C_B of zero measure onto a Cantor set of positive measure C_A.

All the properties listed above remain valid locally for $\hat{F} : \mathbb{R}^n \to \mathbb{R}^n$ defined by

$$\hat{F}(x) = \begin{cases} F(x), & \text{if } x \in [-1,1]^n \\ x, & \text{if } x \in \mathbb{R}^n \backslash [-1,1]^n. \end{cases}$$

Finally, we define $f : \mathbb{R}^n \to \mathbb{R}^n$ by

$$f := \hat{F} \circ g \circ \omega\,.$$

Then it is easy to see that f is a continuous, discrete and open mapping such that

$$f(\mathcal{B}_f) = \hat{F} \circ g((0,0) \times \mathbb{R}^{n-2}) \supset \hat{F}(C_B) = C_A.$$

Therefore it suffices to show that f has finite distortion and satisfies the conditions (1)–(4):

Condition (1): Since $h := g \circ \omega$ defines a quasiregular map there exists $\alpha > 0$ such that $J_h^{-\alpha} \in L^1_{\mathrm{loc}}(\mathbb{R}^n)$, see [29, Remark VI.4.6]. For given $1 \le p < n$ we choose $p < q < n$ such that $\frac{(n-q)p}{(q-p)n} = \alpha$. It is easy to see that h is locally bi-Lipschitz outside the set $A := \{(0,0)\} \times \mathbb{R}^{n-2}$ of zero measure, and thus we know that f is ACL and that the chain rule applies outside the set A. Suppose now that $E \subset \mathbb{R}^n$ is a bounded open set. Then by applying the chain rule on the set $E\backslash A$ we get

$$\begin{aligned}
\int_E |Df|^p &= \int_{E\backslash A} |Df|^p \le \int_{E\backslash A} |D(F\circ h)|^p |Dh|^p = \int_{E\backslash A} |DF(h(x))|^p \, J_h(x)^{\frac{p}{q}} \frac{|Dh(x)|^p}{J_h(x)^{\frac{p}{q}}} \,\mathrm{d}x \\
&\le \left(\int_{E\backslash A} |DF(h(x))|^q \, J_h(x) \,\mathrm{d}x \right)^{\frac{p}{q}} \left(\int_{E\backslash A} \left(\frac{|Dh(x)|^p}{J_h(x)^{\frac{p}{q}}} \right)^{\frac{q}{q-p}} \mathrm{d}x \right)^{\frac{q-p}{q}} \\
&\le K_h^{\frac{p}{n}} \left(\int_{E\backslash A} |DF(h(x))|^q \, J_h(x) \,\mathrm{d}x \right)^{\frac{p}{q}} \left(\int_{E\backslash A} [J_h(x)^{-1}]^{\frac{(n-q)p}{(q-p)n}} \mathrm{d}x \right)^{\frac{q-p}{q}} \\
&\le K_h^{\frac{p}{n}} \left(N(h, E\backslash A) \int_{h(E\backslash A)} |DF(y)|^q \,\mathrm{d}x \right)^{\frac{p}{q}} \left(\int_{E\backslash A} [J_h(x)^{-1}]^{\frac{(n-q)p}{(q-p)n}} \mathrm{d}x \right)^{\frac{q-p}{q}} \\
&= K_h^{\frac{p}{n}} \left(N(h, E\backslash A) \int_{h(E\backslash A)} |DF(y)|^q \,\mathrm{d}x \right)^{\frac{p}{q}} \left(\int_{E\backslash A} J_h(x)^{-\alpha} \mathrm{d}x \right)^{\frac{q-p}{q}} < \infty \,,
\end{aligned}$$

which implies that $f \in W^{1,p}_{\mathrm{loc}}(\mathbb{R}^n, \mathbb{R}^n)$.

Condition (2): We show next that f has finite distortion. Firstly by applying the chain rule we find out that

$$Df(x) = DF(h(x))\, Dh(x) \quad \text{and} \quad J_f(x) = J_F(h(x))\, J_h(x) \tag{3.3}$$

for all $x \in \mathbb{R}^n\backslash A$. Since h is a quasiregular mapping, it satisfies Lusin's condition (N^{-1}) and it follows from (3.3) and from the fact that F is a mapping of finite distortion that $J_f(x) > 0$ almost everywhere in the set $|Df(x)| > 0$. Moreover,

$$\int_E J_f = \int_{E\backslash A} J_f = \int_{E\backslash A} J_F(h(x)) J_h(x) \,\mathrm{d}x \le N(h, E) \int_{h(E\backslash A)} J_F < \infty \,.$$

Thus, f is a mapping of finite distortion.

Next, suppose $\alpha > 1$ is the exponent we defined at the beginning of Condition (1) for which $J_h^{-\alpha} \in L^1_{\mathrm{loc}}(\mathbb{R}^n)$. Set $p_0 = 1 + \frac{1}{\alpha} > 1$ and we get $J_h^{-1/(p_0-1)} \in L^1_{\mathrm{loc}}(\mathbb{R}^n)$. By using the property (c) of the mapping F and concavity of Ψ we obtain

$$\begin{aligned}
&\int_U \exp(\Psi(K_O(x,f))) \,\mathrm{d}x \le \int_U \exp(\Psi(K_O(h(x),F)K_h)) \left(\frac{J_h(x)}{J_h(x)} \right)^{\frac{1}{p_0}} \mathrm{d}x \\
&\le \left(\int_U \exp\big(p_0 \, \Psi(K_O(h(x),F)K_h)\big) \, J_h(x) \,\mathrm{d}x \right)^{\frac{1}{p_0}} \left(\int_U J_h(x)^{-1/(p_0-1)} \,\mathrm{d}x \right)^{\frac{p_0-1}{p_0}} \\
&\le N(h,U)^{\frac{1}{p_0}} \left(\int_{h^{-1}(U)} \exp\big(p_0 K_h \, \Psi(K_O(y,F))\big) \,\mathrm{d}y \right)^{\frac{1}{p_0}} \left(\int_U J_h(x)^{-1/(p_0-1)} \,\mathrm{d}x \right)^{\frac{p_0-1}{p_0}} < \infty \,,
\end{aligned}$$

for every $U \subset\subset \mathbb{R}^n$.

Condition (3): Next, set $\Psi^*(t) := \Psi\big(t^{1/(n-1)}\big)$. Then by the pointwise inequality $K_I(x,f) \le K_O(x,f)^{n-1}$ and by Condition (2) we get

$$\int_U \exp\big(\Psi^*(K_I(x,f))\big)\,\mathrm{d}x \le \int_U \exp\big(\Psi(K_O(x,f))\big)\,\mathrm{d}x < \infty\,,$$

as desired.

Condition (4): We know that h is differentiable almost everywhere, F is differentiable almost everywhere and that h satisfies the Lusin (N^{-1}) condition. It thus follows from (3.3) that f is differentiable almost everywhere. Similarly we obtain from (3.3) that $J_f > 0$ almost everywhere as this holds for both h and F.

Condition (5): Now we observe that $\mathcal{B}_f = \{(0,0)\} \times \mathbb{R}^{n-2}$ and thus

$$\mathcal{L}^n(\mathcal{B}_f) = \mathcal{L}^n(\{(0,0)\} \times \mathbb{R}^{n-2}) = 0\,.$$

On the other hand, it holds that $f(\mathcal{B}_f) \supset C_A$, and therefore

$$\mathcal{L}^n(f(\mathcal{B}_f)) \ge \mathcal{L}^n(C_A) > 0\,,$$

which ends the proof. □

Proof of Theorem 1.4. It is well-known that assumptions of (i) imply that f is continuous, sense-preserving, discrete and open, differentiable almost everywhere and satisfies Lusin condition (N) (see [21]). It follows from Lemma 3.1 that $\mathcal{L}^n(f(\mathcal{B}_f)) = 0$.

The statement of (ii) follows from Theorem 3.2 if we choose $\Psi(t) = \frac{t}{\log^{1+\varepsilon}(e+t)}$ for t large enough. □

4. Proof of Theorem 1.2: the size of $\mathcal{B}_f$

Proof of Theorem 1.2. As we have already pointed out, if a continuous, discrete and open mapping is both

(1) differentiable almost everywhere, and
(2) having non vanishing Jacobian almost everywhere

then the branch set of the mapping has measure zero (see [29, Lemma I.4.11]). The claim of (i) follows as we know from [22] that $K_I(\cdot, f) \in L^1_{\mathrm{loc}}(\Omega)$ implies $J_f > 0$ almost everywhere and from [31] we know that every continuous, discrete and open mapping of finite distortion $f \in W^{1,n-1}_{\mathrm{loc}}(\Omega, \mathbb{R}^n)$ with locally integrable inner distortion function is differentiable almost everywhere.

To prove part (ii) let us define Cantor sets $C_A := C[\{a_k\}_{k=0}^{\infty}]$ and $C_B := C[\{b_k\}_{k=0}^{\infty}]$ by setting

$$a_k := \frac{1}{2}\big(1 + 2^{-k\beta}\big) \quad \text{and} \quad b_k = 2^{-k\beta}\,,$$

where $\beta \ge n+1$. Then it follows that

$$\mathcal{L}^n(C_A) = 1 \quad \text{and} \quad \mathcal{L}^n(C_B) = 0.$$

Suppose that F is the homeomorphism which maps C_A onto C_B and takes each annulus $Q'_{\boldsymbol{v}} \setminus Q_{\boldsymbol{v}}$ radially onto the corresponding annulus $\tilde{Q}'_{\boldsymbol{v}} \setminus \tilde{Q}_{\boldsymbol{v}}$ (see section 2.6 for

details). Then in the interior of each annulus $Q'_{\boldsymbol{v}} \setminus Q_{\boldsymbol{v}}$ we get by applying (2.6) and (2.7) that

$$|DF(x)| \sim \max\left\{\frac{b_k}{a_k}, \frac{b_{k-1}-b_k}{a_{k-1}-a_k}\right\} \sim \max\left\{2^{-k\beta}, 1\right\} = 1 \quad \text{and} \quad |D^\sharp F(x)| \sim 2^{-k\beta(n-2)}.$$

In addition, we also have

$$J_F(x) \sim \left(\frac{b_k}{a_k}\right)^{n-1} \frac{b_{k-1}-b_k}{a_{k-1}-a_k} \sim (2^{-k\beta})^{n-1}\,.$$

Hence

$$K_O(x,F) = \frac{|Df(x)|^n}{J_f(x)} \sim (2^{k\beta})^{n-1} \quad \text{and} \quad K_I(x,F) = \frac{|D^\sharp f(x)|^n}{J_f(x)^{n-1}} \sim 2^{k\beta}.$$

It follows that F is Lipschitz and if $0 < p < \frac{1}{n-1}$ then

$$\begin{aligned}\int_{Q_0} K_O(x,F)^p \,\mathrm{d}x &\le C\sum_{k=1}^{\infty} 2^{kn}2^{-kn}a_k^{n-1}(a_k - a_{k+1})(2^{k\beta})^{(n-1)p} \\ &\le C\sum_{k=1}^{\infty} 2^{kn}2^{-kn}1^{n-1}2^{-k\beta}(2^{k\beta})^{(n-1)p} < \infty\,,\end{aligned} \tag{4.1}$$

and similarly for every $0 < q < 1$ we get

$$\begin{aligned}\int_{Q_0} K_I(x,F)^q \,\mathrm{d}x &\le C\sum_{k=1}^{\infty} 2^{kn}2^{-kn}a_k^{n-1}(a_k - a_{k+1})(2^{k\beta})^{q} \\ &\le C\sum_{k=1}^{\infty} 2^{kn}2^{-kn}1^{n-1}2^{-k\beta}(2^{k\beta})^{q} < \infty\,.\end{aligned} \tag{4.2}$$

Suppose next $g : \mathbb{R}^n \to \mathbb{R}^n$ is the bi-Lipschitz mapping (defined in section 2.8) which takes the Cantor set C_B onto the Cantor's tower C_B^T. Furthermore, let $\omega : \mathbb{R}^n \to \mathbb{R}^n$ be the winding map. Then both mappings g and ω are quasiregular and therefore there exist constants $K_g \ge 1$ and $K_\omega \ge 1$ such that

$$|Dg(x)|^n \le K_g J_g(x) \quad \text{and} \quad |D\omega(x)|^n \le K_\omega J_\omega(x) \tag{4.3}$$

for almost every x. We also have

$$|D^\sharp g(x)|^n \le K_g^{n-1} J_g(x)^{n-1} \quad \text{and} \quad |D^\sharp \omega(x)|^n \le K_\omega^{n-1} J_\omega(x)^{n-1} \tag{4.4}$$

for almost every x.

Now we define the mapping $f : \mathbb{R}^n \to \mathbb{R}^n$ as

$$f := \omega \circ g \circ F\,.$$

Then F maps C_A onto C_B which is mapped by g into the segment $\{0\}^{n-1} \times [-1,1]$. Since ω is winding around this segment, all points on this segment belong to the branch set. The branch set of f thus contains the whole set C_A and we get $\mathcal{L}^n(\mathcal{B}_f) > 0$.

Furthermore, f is a Lipschitz mapping as a composition of three Lipschitz mappings. It is easy to see that $|DF(x)| = 0$ and $J_F(x) = 0$ for almost every $x \in C_A$ and

the composition with Lipschitz mapping cannot change this. Hence $|Df(x)| = 0$ and $J_f(x) = 0$ for almost every $x \in C_A$ and consequently

$$K_O(x, f) = 1 \quad \text{for almost every } x \in C_A. \tag{4.5}$$

With a similar way we may also show that

$$K_I(x, f) = 1 \quad \text{for almost every } x \in C_A. \tag{4.6}$$

Moreover, F is locally bi-Lipschitz outside of C_A and hence preimages of sets (outside of C_A) of zero measure have zero measure. It follows that g has classical derivative at $F(x)$ for almost every $x \notin C_A$ (as the preimage under F of points of non-differentiability of g has zero measure). As g is bi-Lipschitz we can argue similarly to deduce that the derivative of ω exists at a point $g(F(x))$ for almost every $x \notin C_A$. By the chain rule we obtain that for almost every $x \notin C_A$ we have

$$|Df(x)| = |D\omega(g(F(x)))|\,|Dg(F(x))|\,|DF(x)|, \text{ and} \tag{4.7}$$

$$|D^\sharp f(x)| = |D^\sharp\omega(g(F(x)))|\,|D^\sharp g(F(x))|\,|D^\sharp F(x)|. \tag{4.8}$$

In addition, we also get

$$J_f(x) = J_\omega(g(F(x)))\, J_g(F(x))\, J_F(x)\ . \tag{4.9}$$

It follows from (4.3)–(4.9) that

$$K_O(x, f) \le \frac{|Df(x)|^n}{J_f(x)} \le K_\omega K_g\, \frac{|DF(x)|^n}{J_F(x)}, \text{ and} \tag{4.10}$$

$$K_I(x, f) \le \frac{|D^\sharp f(x)|^n}{J_f(x)^{n-1}} \le K_\omega^{n-1} K_g^{n-1}\, \frac{|D^\sharp F(x)|^n}{J_F(x)^{n-1}} \tag{4.11}$$

for almost every $x \in Q_0 \setminus C_A$. Finally, by (4.5), (4.10) and (4.1) we conclude $K_O(\cdot, f) \in L^p_{\mathrm{loc}}(Q_0)$ for all $0 < p < \frac{1}{n-1}$. Similarly, by (4.6), (4.10) and (4.2) we conclude that $K_I(\cdot, f) \in L^q_{\mathrm{loc}}(Q_0)$ for all $0 < q < 1$. □

5. Mapping of a Cantor set onto a Cantor set which maps corners onto corners

Before coming to the proof of Theorem 1.3 we need to construct a special homeomorphism which maps a Cantor set of positive measure onto a Cantor set of zero measure such that the corners of the first construction are mapped close to the corners of the second construction. Here by corners we mean the part of the cubes $Q'_{\boldsymbol{v}(k)} \setminus Q_{\boldsymbol{v}(k)}$ that are close to edges and vertices (see Fig. 8), the formal definition is given later. Let us note that the standard construction (see the mapping g in section 2.6) is not good for us as the (relatively small) corners of the first Cantor construction are not mapped onto (relatively big) corners of the second Cantor construction. We have to define the mapping close to the vertices so that it is stretching much more there.

Let us define the Cantor sets $C_A := C[\{a_k\}_{k=0}^\infty]$ and $C_B := C[\{b_k\}_{k=0}^\infty]$ by setting

$$a_k = \frac{1}{2}\Big(1 + \frac{1}{2^k}\Big) \quad \text{and} \quad b_k = 2^{-k\beta}, \tag{5.1}$$

where $\beta \geq n+1$. Then

$$\mathcal{L}^n(C_A) = \lim_{k\to\infty} 2^{nk}(2a_k 2^{-k})^n = \lim_{k\to\infty} \Big(1+\frac{1}{2^k}\Big)^n = 1$$

and

$$\mathcal{L}^n(C_B) = \lim_{k\to\infty} 2^{nk}(2b_k 2^{-k})^n = \lim_{k\to\infty} 2^{-kn\beta} = 0\,.$$

5.1. **Planar case.** For simplicity and comprehensibility we give the details of the construction only for $n = 2$ and then we briefly explain the differences in higher dimensions. Set

$$r_k = 2^{-k}a_k \quad \text{and} \quad \tilde{r}_k = 2^{-k}b_k\,, \tag{5.2}$$

and recall that the cubes in the definition of the Cantor set C_A (see section 2.5) are defined as

$$Q'_{\boldsymbol{v}(k)} = Q\Big(z_{\boldsymbol{v}(k)}, \frac{r_{k-1}}{2}\Big) \quad \text{and} \quad Q_{\boldsymbol{v}(k)} = Q(z_{\boldsymbol{v}(k)}, r_k).$$

For simplicity assume that $z_{\boldsymbol{v}(k)} = (0,0)$. Then we define the corners G_k and sides S_k of the annulus $Q'_{\boldsymbol{v}(k)} \setminus Q_{\boldsymbol{v}(k)}$ as follows (see Fig. 5): we project vertices of $Q_{\boldsymbol{v}(k)}$ onto sides of $Q'_{\boldsymbol{v}(k)}$ and we get points

$$(\pm r_k, \pm\tfrac{r_{k-1}}{2}) \text{ and } (\pm\tfrac{r_{k-1}}{2}, \pm r_k).$$

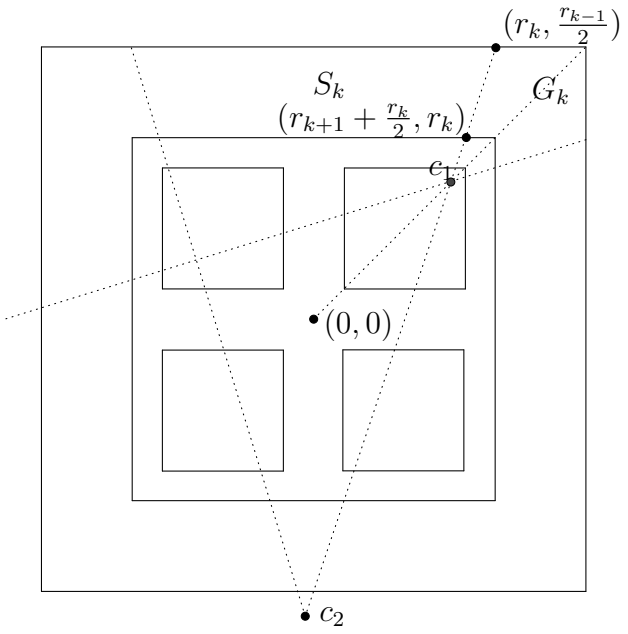

Fig. 5 Construction of corners in dimension $n = 2$

Analogously we project vertices of four smaller cubes $Q_{\boldsymbol{v}(k+1)}$ onto $\partial Q'_{\boldsymbol{v}(k+1)}$ and we get points

$$\big(\pm(r_{k+1}+\tfrac{r_k}{2}), \pm r_k\big) \text{ and } \big(\pm r_k, \pm(r_{k+1}+\tfrac{r_k}{2})\big).$$

We connect the corresponding eight pairs of points (e.g. we connect $(r_k, \frac{r_{k-1}}{2})$ with $(r_{k+1}+\frac{r_k}{2}, r_k)$). In this way we divide the annulus $Q'_{\boldsymbol{v}(k)} \setminus Q_{\boldsymbol{v}(k)}$ into eight parts and

we call G_k the four parts that contain the vertices and S_k the other four parts along the sides (see Fig. 5).

Analogously define the division of $\tilde{Q}'_{\boldsymbol{v}(k)} \setminus \tilde{Q}_{\boldsymbol{v}(k)}$ corresponding to the construction of a Cantor set C_B and we divide this annulus into parts $\tilde{G}_k$ and $\tilde{S}_k$. Our aim is to construct a mapping g which maps parts G_k onto corresponding parts $\tilde{G}_k$ and parts S_k onto corresponding parts $\tilde{S}_k$. In this way g maps the corners G_k of the first Cantor construction onto corners $\tilde{G}_k$ of the second Cantor type construction. The mapping that maps G_k onto $\tilde{G}_k$ is in fact given by a formula

$$\frac{x}{\|x\|}(\alpha\|x\| + \beta)$$

similarly as in (2.4). The difference is that now the mapping will be radial (in supremum norm) with respect to different centers. The role of center in the domain will play the point c_1 in Fig. 5 and the role of the center in the domain is the corresponding point $\tilde{c}_1$ in the image (see Fig. 6).

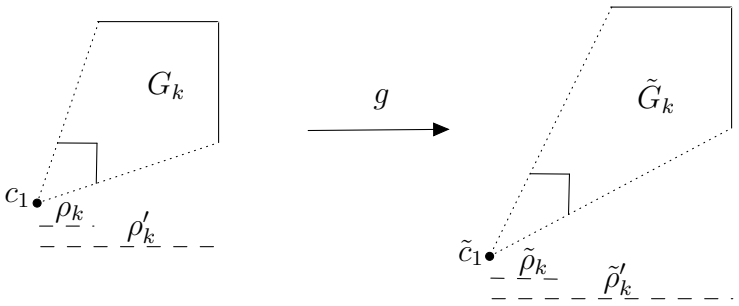

Fig. 6 Mapping of a corner onto another corner for $n = 2$

We define g by

$$g(x - c_1) = \tilde{c}_1 + (\alpha_k\|x - c_1\| + \beta_k)\frac{x - c_1}{\|x - c_1\|} \quad \text{for } x \in G_k\,, \tag{5.3}$$

where $\alpha_k,\ \beta_k,\ \gamma_k$ and δ_k are defined so that (see Fig. 6)

$$\alpha_k\rho_k + \beta_k = \tilde{\rho}_k \quad \text{and} \quad \alpha_k\rho'_k + \beta_k = \tilde{\rho}'_k\,. \tag{5.4}$$

This choice implies that the mapping is continuous and has correct boundary values. Since g is affine on

$$S_k \cap \partial\tilde{Q}'_{\boldsymbol{v}(k)},\ G_k \cap \tilde{Q}'_{\boldsymbol{v}(k)},\ S_k \cap \tilde{Q}_{\boldsymbol{v}(k)} \text{ and } G_k \cap \tilde{Q}_{\boldsymbol{v}(k)}$$

it is easy to see that the definition for k and $k+1$ from top and bottom agree on the boundary. Let us also note that in (5.3) we obviously have different c_1 and $\tilde{c}_1$ for four different parts of G_k (upper right, upper left, lower right and lower right).

Similarly let c_2 and $\tilde{c}_2$ (see Fig. 5) be the centers corresponding to mapping S_k onto $\tilde{S}_k$ and we define

$$g(x - c_2) = \tilde{c}_2 + (\gamma_k\|x - c_2\| + \delta_k)\frac{x - c_2}{\|x - c_2\|} \text{ for } x \in S_k\,,$$

where γ_k and δ_k are again chosen so that the mapping has correct boundary values, i.e., (see Fig. 7)

$$\gamma_k\lambda_k + \delta_k = \tilde{\lambda}_k \quad \text{and} \quad \gamma_k\lambda_k' + \delta_k = \tilde{\lambda}_k'. \tag{5.5}$$

It is not difficult to see that in this way our mapping g is a homeomorphism by a similar reasoning as in section 2.2.

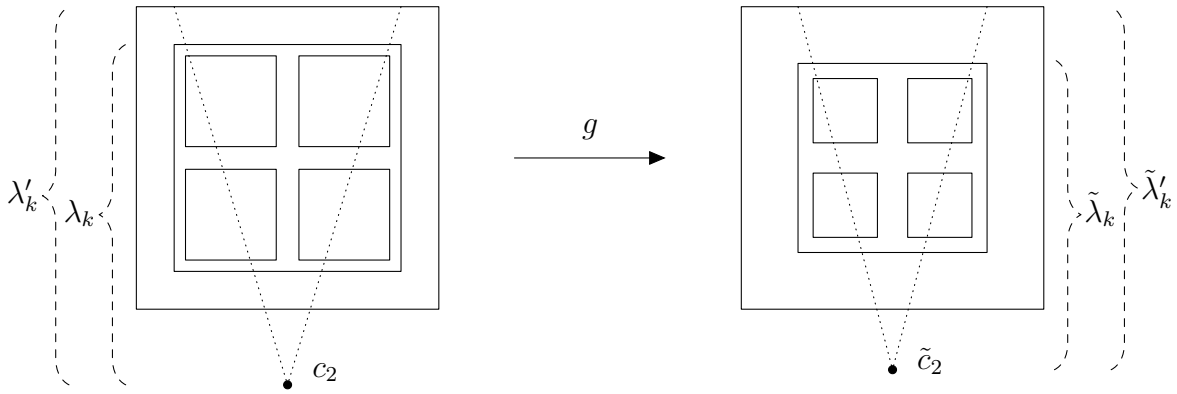

Fig. 7 Mapping of a side onto another side for $n = 2$

Now we compute the exact position of c_1, c_2, determine parameters α_k, β_k, γ_k and δ_k and estimate the derivatives of g. Let us denote by $y = ax + b$ the line that connects $(r_k, \frac{r_{k-1}}{2})$ with $(r_{k+1} + \frac{r_k}{2}, r_k)$ (recall that $z_{\boldsymbol{v}(k)} = 0$), i.e.,

$$\tfrac{r_{k-1}}{2} = ar_k + b \text{ and } r_k = a(r_{k+1} + \tfrac{r_k}{2}) + b.$$

An easy computation leads to

$$a = \frac{\frac{r_{k-1}}{2} - r_k}{\frac{r_k}{2} - r_{k+1}} = 2\frac{a_{k-1} - a_k}{a_k - a_{k+1}} = 4 \text{ and } b = \frac{r_{k-1}}{2} - 4r_k = -\frac{3}{2^{k+1}} - \frac{1}{2^{2k}}. \tag{5.6}$$

We obtain the coordinates of c_1 by finding intersection of lines $y = x$ and $y = ax + b$ and we have

$$c_1 = \Big(\frac{1}{2^{k+1}} + \frac{1}{3\cdot 2^{2k}}, \frac{1}{2^{k+1}} + \frac{1}{3\cdot 2^{2k}}\Big).$$

Similarly we obtain from

$$\tfrac{\tilde{r}_{k-1}}{2} = \tilde{a}\tilde{r}_k + \tilde{b} \text{ and } \tilde{r}_k = \tilde{a}(\tilde{r}_{k+1} + \tfrac{\tilde{r}_k}{2}) + \tilde{b}$$

that

$$\tilde{a} = 2^{1+\beta},\ \tilde{b} = \frac{-1}{2^{k+(k-1)\beta}} \text{ and } \tilde{c}_1 = \Big(\frac{1}{(2^{\beta+1}-1)2^{k+(k-1)\beta}}, \frac{1}{(2^{\beta+1}-1)2^{k+(k-1)\beta}}\Big).$$

Knowing c_1 and $\tilde{c}_1$ it is easy to see (see Fig. 6) that

$$\rho_k = r_k - \frac{1}{2^{k+1}} - \frac{1}{3\cdot 2^{2k}}, \quad \rho_k' = \frac{r_{k-1}}{2} - \frac{1}{2^{k+1}} - \frac{1}{3\cdot 2^{2k}},$$
$$\tilde{\rho}_k = \tilde{r}_k - \frac{1}{(2^{\beta+1}-1)2^{k+(k-1)\beta}} \quad \text{and} \quad \tilde{\rho}_k' = \frac{\tilde{r}_{k-1}}{2} - \frac{1}{(2^{\beta+1}-1)2^{k+(k-1)\beta}}.$$

For $x \in G_k$ we have

$$\alpha_k\|x-c_1\|+\beta_k \sim \tilde{\rho}_k \sim 2^{-k-k\beta} \text{ and } \|x-c_1\| \sim \rho_k \sim 2^{-2k}$$

and by (5.4) it follows that

$$\alpha_k = \frac{\tilde{\rho}'_k - \tilde{\rho}_k}{\rho'_k - \rho_k} \sim \frac{2^{-k-k\beta}}{2^{-2k}} = 2^{k-k\beta}.$$

By Lemma 2.3 we obtain that for $x \in G_k$ we have

$$|Dg(x)| \sim \max\left\{\alpha_k, \frac{\alpha_k\|x-c_1\|+\beta_k}{\|x-c_1\|}\right\} \sim \max\left\{2^{k-k\beta}, \frac{2^{-k-k\beta}}{2^{-2k}}\right\} = 2^{k-k\beta} \tag{5.7}$$

and as (here $n=2$ but similar estimate holds for other n)

$$J_f(x) \sim \alpha_k\Big(\frac{\alpha_k\|x-c_1\|+\beta_k}{\|x-c_1\|}\Big)^{n-1} \sim 2^{n(k-k\beta)} \text{ we have } K_O(x,g) \sim 1. \tag{5.8}$$

Similarly the point c_2 lies on $y=ax+b$ for $x=0$ and we have

$$c_2 = \Big(0, -\frac{3}{2^{k+1}} - \frac{1}{2^{2k}}\Big) \text{ and } \tilde{c}_2 = \Big(0, \frac{-1}{2^{k+(k-1)\beta}}\Big).$$

Knowing c_2 and $\tilde{c}_2$ it is easy to see (see Fig. 7) that

$$\lambda_k = r_k + \frac{3}{2^{k+1}} + \frac{1}{2^{2k}}, \quad \lambda'_k = \frac{r_{k-1}}{2} + \frac{3}{2^{k+1}} + \frac{1}{2^{2k}}$$
$$\tilde{\lambda}_k = \tilde{r}_k + \frac{1}{2^{k+(k-1)\beta}} \quad \text{and} \quad \tilde{\lambda}'_k = \frac{\tilde{r}_{k-1}}{2} + \frac{1}{2^{k+(k-1)\beta}}.$$

Analogous computation as above gives that for $x \in S_k$ we have

$$\gamma_k\|x-c_2\|+\delta_k \sim \tilde{\lambda}_k \sim 2^{-k-k\beta}, \ \|x-c_2\| \sim \lambda_k \sim 2^{-k},$$

and by (5.5) we get

$$\gamma_k \sim \frac{\tilde{\lambda}'_k - \tilde{\lambda}_k}{\lambda'_k - \lambda_k} \sim \frac{2^{-k-k\beta}}{2^{-2k}} = 2^{k-k\beta}.$$

It follows by Lemma 2.3 that for $x \in S_k$ we have

$$|Dg(x)| \sim \max\left\{2^{k-k\beta}, \frac{2^{-k-k\beta}}{2^{-k}}\right\} = 2^{k-k\beta}, \tag{5.9}$$
$$J_g(x) \sim 2^{k-k\beta}\big(2^{-k\beta}\big)^{n-1} \quad \text{and} \quad K_O(x,g) \sim 2^{k(n-1)}.$$

5.2. **Higher dimensions.** Now let us briefly explain the differences of the construction for $n=3$. Again for simplicity assume that $z_{\boldsymbol{v}(k)}=0$ and let us concentrate on the first octant

$$\{(x_1,x_2,x_3) \in (-1,1)^3 : \ x_1 \geq 0, x_2 \geq 0, x_3 \geq 0\}.$$

We consider planes (see Fig. 5)

$x_2 = ax_1+b$, $x_1 = ax_2+b$, $x_3 = ax_1+b$, $x_1 = ax_3+b$, $x_2 = ax_3+b$ and $x_3 = ax_2+b$,

where a, b are the same as in (5.6). We consider similar planes in other octants and these planes will divide $Q'_{\boldsymbol{v}(k)} \setminus Q_{\boldsymbol{v}(k)}$ into $8+6+12=26$ parts. Eight of these parts contains a vertex of $Q_{\boldsymbol{v}(k)}$ and we call them again G_k. Six of these parts contains centers of faces of $Q_{\boldsymbol{v}(k)}$ (and big part of the face itself) and we call them S_k. Finally

the remaining twelve parts contain centers of edges of $Q_{\boldsymbol{v}(k)}$ (and big part of the edge itself) and we call them E_k.

Similarly we divide $\tilde{Q}'_{\boldsymbol{v}(k)} \setminus \tilde{Q}_{\boldsymbol{v}(k)}$ into 26 parts and we would like to map corresponding parts onto corresponding parts. For mapping G_k onto $\tilde{G}_k$ we consider points (of course with corresponding $\pm$ signs for different vertices of $Q_{\boldsymbol{v}(k)}$)

$$c_1 = \Big(\frac{1}{2^{k+1}} + \frac{1}{3\cdot 2^{2k}}, \frac{1}{2^{k+1}} + \frac{1}{3\cdot 2^{2k}}, \frac{1}{2^{k+1}} + \frac{1}{3\cdot 2^{2k}}\Big)$$

and

$$\tilde{c}_1 = \Big(\frac{1}{(2^{\beta+1}-1)2^{k+(k-1)\beta}}, \frac{1}{(2^{\beta+1}-1)2^{k+(k-1)\beta}}, \frac{1}{(2^{\beta+1}-1)2^{k+(k-1)\beta}}\Big).$$

The mapping

$$g(x-c_1) = \tilde{c}_1 + (\alpha_k\|x-c_1\| + \beta_k)\frac{x-c_1}{\|x-c_1\|} \text{ for } x \in G_k$$

works exactly as before and maps G_k onto $\tilde{G}_k$ and all the estimates (5.7) and (5.8) remain valid.

Similarly for parts S_k we define points

$$c_2 = \Big(0, 0, -\frac{3}{2^{k+1}} - \frac{1}{2^{2k}}\Big) \text{ and } \tilde{c}_2 = \Big(0, 0, \frac{-1}{2^{k+(k-1)\beta}}\Big)$$

(and corresponding permutations and signs for different faces) and we define

$$g(x-c_2) = \tilde{c}_2 + (\gamma_k\|x-c_2\| + \delta_k)\frac{x-c_2}{\|x-c_2\|} \text{ for } x \in S_k.$$

As before we obtain (5.9). It is not difficult to see that this mapping is continuous on $G_k \cap S_k$ and on other parts where it is defined.

It remains to consider parts E_k that correspond to edges of $Q_{\boldsymbol{v}(k)}$. Let us consider for example the edge from (r_k, r_k, r_k) to $(-r_k, r_k, r_k)$. This part of the set E_k intersects two corners G_k, in fact it has a common face with those two corner sets. Let us call these faces A and $\hat{A}$. It is easy to see that these two faces are the same up to a translation and rotation and hence for every $x \in A$ we can find a corresponding point $\hat{a} \in \hat{A}$. Since g is already defined on those two faces (by the definition on G_k) we can define

$$g(tx + (1-t)\hat{x}) = tg(x) + (1-t)g(\hat{x}) \text{ for every } t \in [0,1]. \tag{5.10}$$

As each point in E_k can be written as such a convex combination we have defined g on E_k. It is not difficult to see that this g is continuous on $E_k \cap G_k$ and $E_k \cap S_k$ and that we obtain a homeomorphism. It remains to estimate its derivatives. Both derivatives along A (or $\hat{A}$) are comparable to $2^{k-\beta k}$ as in (5.7). The derivative in the t-direction (see (5.10)) is comparable to the ratio of side lengths of $Q_{\boldsymbol{v}(k)}$ and $\tilde{Q}_{\boldsymbol{v}(k)}$ and hence it is comparable to $\frac{2^{-k-k\beta}}{2^{-k}} = 2^{-k\beta}$. It follows that on E_k we have

$$|Dg(x)| \sim 2^{k-\beta k},\ J_g(x) \sim 2^{2(k-\beta k)}2^{-\beta k} \quad \text{and} \quad K_O(x,g) \sim 2^k, \tag{5.11}$$

and also

$$|D^\sharp g(x)| \sim 2^{2(k-\beta k)} \quad \text{and} \quad K_I(x,g) \sim 2^{2k} \tag{5.12}$$

To sum up the estimates close to d-dimensional faces (set $d = 2$ for S_k, $d = 1$ for E_k and $d = 0$ for G_k) of the cubes we have

(5.13)

$$|Dg(x)| \sim \begin{cases} 2^{k-\beta k}, & \text{if } x \in G_k \\ 2^{k-\beta k}, & \text{if } x \in E_k \\ 2^{k-\beta k}, & \text{if } x \in S_k \end{cases}, \quad J_g(x) \sim \begin{cases} 2^{3(k-\beta k)}, & \text{if } x \in G_k \\ 2^{2(k-\beta k)}2^{-\beta k}, & \text{if } x \in E_k \\ 2^{k-\beta k}2^{-2\beta k}, & \text{if } x \in S_k \end{cases} \text{ and}$$

$$|D^\sharp g(x)| \sim \begin{cases} 2^{2(k-\beta k)}, & \text{if } x \in G_k \\ 2^{2(k-\beta k)}, & \text{if } x \in E_k \\ 2^{k-\beta k}2^{-\beta k}, & \text{if } x \in S_k, \end{cases}$$

and also

$$K_O(x,g) \sim \begin{cases} 1, & \text{if } x \in G_k \\ 2^k, & \text{if } x \in E_k \\ 2^{2k}, & \text{if } x \in S_k \end{cases} \quad \text{and} \quad K_I(x,g) \sim \begin{cases} 1, & \text{if } x \in G_k \\ 2^{2k}, & \text{if } x \in E_k \\ 2^k, & \text{if } x \in S_k. \end{cases} \tag{5.14}$$

Similarly we can estimate the derivative of the inverse:

(5.15)

$$|Dg^{-1}(y)| \sim \begin{cases} 2^{\beta k-k}, & \text{if } y \in \tilde{G}_k \\ 2^{\beta k}, & \text{if } y \in \tilde{E}_k \\ 2^{\beta k}, & \text{if } y \in \tilde{S}_k \end{cases}, \quad J_{g^{-1}}(y) \sim \begin{cases} 2^{3(\beta k-k)}, & \text{if } \in \tilde{G}_k \\ 2^{2(\beta k-k)}2^{\beta k}, & \text{if } y \in \tilde{E}_k \\ 2^{(\beta k-k)}2^{2\beta k}, & \text{if } y \in \tilde{S}_k \end{cases} \text{ and}$$

$$|D^\sharp g^{-1}(y)| \sim \begin{cases} 2^{2(\beta k-k)}, & \text{if } y \in \tilde{G}_k \\ 2^{(\beta k-k)}2^{\beta k}, & \text{if } y \in \tilde{E}_k \\ 2^{2\beta k}, & \text{if } y \in \tilde{S}_k, \end{cases}$$

and for the distortions we have

$$K_O(y,g^{-1}) \sim \begin{cases} 1, & \text{if } \in \tilde{G}_k \\ 2^{2k}, & \text{if } y \in \tilde{E}_k \\ 2^k, & \text{if } y \in \tilde{S}_k \end{cases} \quad \text{and} \quad K_I(y,g^{-1}) \sim \begin{cases} 1, & \text{if } \in \tilde{G}_k \\ 2^k, & \text{if } y \in \tilde{E}_k \\ 2^{2k}, & \text{if } y \in \tilde{S}_k. \end{cases} \tag{5.16}$$

In dimensions $n \geq 4$ it is possible to proceed similarly. We do not need the construction in higher dimension and therefore we will only sketch it. The corresponding hyperplanes $x_i = ax_j + b$ divide $Q'_{\boldsymbol{v}(k)} \setminus Q_{\boldsymbol{v}(k)}$ into parts that correspond to various d-dimensional facets for $d \in \{0, \dots, n-1\}$. We define the mapping as radial (with respect to supremum norm) on corners G_k and on "$(n-1)$-dimensional" faces E_k. Then we use various linear interpolation to define it on the remaining parts. On the parts that correspond to d-dimensional faces we have

$$|Dg(x)| \sim 2^{k-\beta k}, \ J_g(x) \sim 2^{(k-\beta k)(n-d)}2^{-\beta k d} \text{ and } K_O(x,g) \sim 2^{dk}.$$

Similarly we can estimate the derivative of the inverse and we obtain

$$|Dg^{-1}(y)| \sim \begin{cases} 2^{\beta k} & \text{for } d \neq 0 \\ 2^{\beta k-k} & \text{for } d = 0, \end{cases}$$

and further we have

$$J_{g^{-1}}(y) \sim 2^{(-k+\beta k)(n-d)}2^{\beta k d} \quad \text{and} \quad K_O(y,g^{-1}) \sim \begin{cases} 2^{k(n-d)} & \text{for } d \neq 0 \\ 1 & \text{for } d = 0. \end{cases}$$

5.3. **Definition of corners in three dimensions.** In two dimensions we called the sets G_k as corners (see Fig. 5 and Fig. 6). In three dimensions the sets which we will refer as (three dimensional) corners are the sets

$$C_{\boldsymbol{v}(k)} := C_k := G_k \cup E_k, \tag{5.17}$$

where the sets G_k and E_k are defined as in the subsection 5.2.

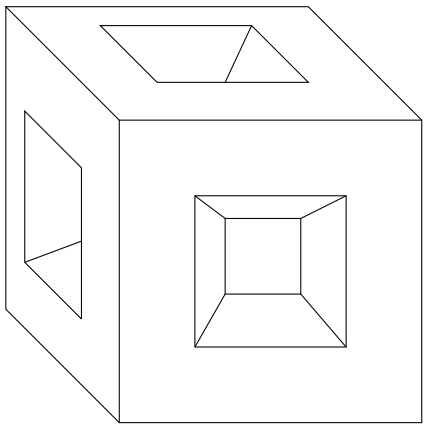

Fig. 8 Three dimensional corner $C_{\boldsymbol{v}(k)}$

It is easy to see that we can use (5.1) and (5.2) to estimate its measure as

$$\mathcal{L}^3(C_{\boldsymbol{v}(k)}) \leq C r_{k-1}(\frac{r_{k-1}}{2} - r_k)^2 \leq C 2^{-5k}$$

and hence

$$\mathcal{L}^3(\bigcup_{\boldsymbol{v}(k)\in\mathbb{V}^k} C_{\boldsymbol{v}(k)}) \leq 2^{3k}\mathcal{L}^3(C_{\boldsymbol{v}(k)}) \leq C 2^{-2k}. \tag{5.18}$$

6. Explicit construction of the bi-Lipschitz map in three dimensions

Let us now consider the Cantor set $C_B := C[\{b_k\}_{k=0}^{\infty}]$ of zero measure defined by the sequence

$$b_k = 2^{-10k},$$

and suppose the Cantor set $C_A := C_A[\{a_k\}_{k=0}^{\infty}]$ is defined as in section 5.

Points in $[-1,1]^3$ we denote in coordinates as (x,y,z). Let $\theta > 0$ be small enough (we give exact condition later) but fixed. We use $\mathcal{S}_\theta$ to denote a specific "sector" of angle θ:

$$\mathcal{S}_\theta := \{x \in \mathbb{R}^n : 1 - \tfrac{\theta}{2} \leq \arctan(y/x) \leq 1 + \tfrac{\theta}{2}\},$$

i.e., $\mathcal{S}_\theta = \{(x,y,z) \in [-1,1]^3 : \ (x,y) \in s_\theta^{xy}\}$ where the set s_θ^{xy} can be seen in the picture below.

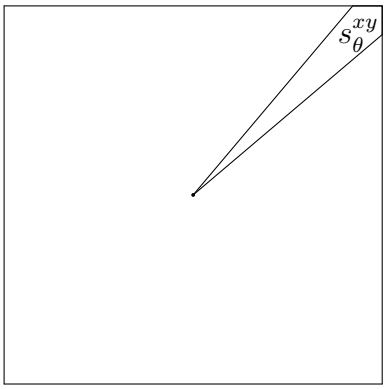

Fig. 9 Definition of sector $\mathcal{S}_\theta$.

Suppose $L : [-1,1]^3 \to [-1,1]^3$ is a given bi-Lipschitz map which takes the Cantor set C_B onto corresponding Cantor's tower C_B^T, and let g be the homeomorphism defined in section 5. Then we define the *set of bad points* (related to mapping L) as

$$\mathbb{BAD}(L) := \big\{x \in (-1,1)^3 : L(g(x)) \in \mathcal{S}_\theta\big\},$$

and for each $k \in \{1,2,\ldots\}$ we define the *set of bad points in k-th step* as

$$\begin{aligned}\mathbb{BAD}_k(L) &:= \Big\{x \in \bigcup_{\boldsymbol{v}(k)\in\mathbb{V}^k} Q'_{\boldsymbol{v}(k)} \setminus Q_{\boldsymbol{v}(k)} : L(g(x)) \in \mathcal{S}_\theta\Big\}\\ &= \Big\{x \in \bigcup_{\boldsymbol{v}(k)\in\mathbb{V}^k} Q'_{\boldsymbol{v}(k)} \setminus Q_{\boldsymbol{v}(k)} : x \in \mathbb{BAD}\Big\}.\end{aligned}$$

Our goal is to find a bi-Lipschitz map $L : [-1,1]^3 \to [-1,1]^3$ such that the following conditions hold:

(1) Mapping L takes C_B onto C_B^T.
(2) We have

$$(L\circ g)^{-1}\left(\mathcal{S}_\theta \cap \left(\hat{Q}'_{\boldsymbol{v}(k)} \setminus \bigcup_{\boldsymbol{v}(k+1)\in\mathbb{V}^{k+1}} \hat{Q}'_{\boldsymbol{v}(k+1)}\right)\right) \subset \bigcup_{\boldsymbol{v}(k)\in\mathbb{V}^k} C_{\boldsymbol{v}(k)}. \tag{6.1}$$

In other words, the preimage $(L\circ g)^{-1}(\mathcal{S}_\theta)$ is contained in the union of the corners. This can be written equivalently as follows:

$$\mathbb{BAD}_k(L) \subset C_{\boldsymbol{v}(k)}.$$

(3) Mapping L maps $\tilde{Q}_{\boldsymbol{v}(k)}$ onto the cube $L(\tilde{Q}_{\boldsymbol{v}(k)})$ of the same size.

We know that corners of C_A are mapped onto corners of C_B by g. Hence our mapping L has to map corners of C_B onto a set which contains $\mathcal{S}_\theta$. Recall that corners are defined in (5.17) (see also Fig. 8) and hence we require that the images of red pipes (in the Fig. 10 below) under mapping L do not intersect $\mathcal{S}_\theta$. We will also prescribe the values of L on the boundaries of $\tilde{Q}_{\boldsymbol{v}}$ so it is easy to glue mappings together.

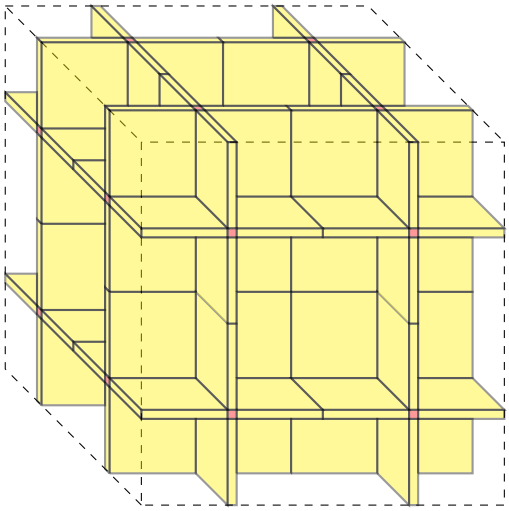

Fig. 10 The sets $\tilde{E}_k$ (yellow slabs), the sets $\tilde{S}_k$ (red pipes) and the sets $\tilde{G}_k$ (empty space between the slabs)

To define the bi-Lipschitz map $L : [-1,1]^3 \to [-1,1]^3$ we first define a bi-Lipschitz map $L_1 : [-1,1]^3 \to [-1,1]^3$ satisfying the conditions (1)–(3) above for $k = 1$. After this we iterate this procedure in the following steps and check that the bi-Lipschitz constant stays the same in all steps of the iteration. Moreover, we also need to check that the boundary values of all the iterations L_k will coincide. We briefly outline this below:

Outline of the construction of the mapping L. Our mapping will be a composition of four bi-Lipschitz mappings

$$L_1 := L_x \circ L_y \circ L_z \circ L_p.$$

The mapping L_p prepares the correct boundary values and it is identity in most places

$$L_p(x,y,z) = (x,y,z) \text{ for every } (x,y,z) \in [-1,1]^2 \times [-1+\tfrac{1}{20}, 1-\tfrac{1}{20}], \tag{6.2}$$

especially it is identity on cubes $\tilde{Q}_{\boldsymbol{v}(1)}$ and in their neighborhood. Furthermore, it moves the small two dimensional red squares on top and bottom of Fig. 10 (corresponding to $z = \pm 1$) to other places so that their image does not intersect $\mathcal{S}_\theta \cap \partial[-1,1]^3$ (more details are given below). Then, we define a mapping L_z which moves 8 cubes $\tilde{Q}_{\boldsymbol{v}(1)}$ in the z-direction so that their z-coordinate becomes

$$\left\{-\frac{7}{8}, -\frac{5}{8}, -\frac{3}{8}, -\frac{1}{8}, \frac{1}{8}, \frac{3}{8}, \frac{5}{8}, \frac{7}{8}\right\}, \tag{6.3}$$

so they correspond to the z-coordinates of the tower formation (see Fig. 3 and Fig. 4) in dimension $n = 3$. The image under L_z of $\tilde{Q}_{\boldsymbol{v}(1)}$ and red pipes from Fig. 10 is shown in Fig. 11 below (we show the projection to xz-plane). It is easy to see that the projections of $L_z(\tilde{Q}_{\boldsymbol{v}(1)})$ to z-coordinate are disjoint and far away (their size is in fact much smaller than on this sketch).

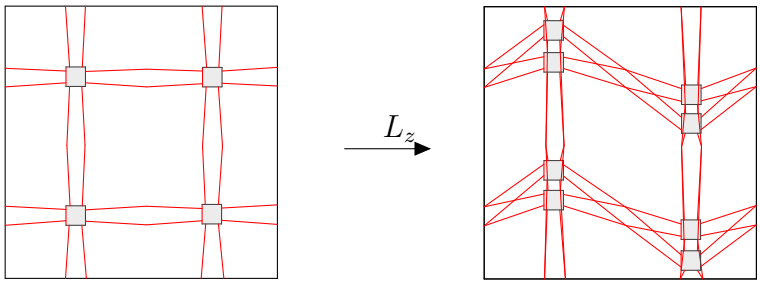

Fig. 11 L_z maps z coordinates of $\tilde{Q}_{\boldsymbol{v}(1)}$ to tower formation (projection to xz-plane)

Then the mapping L_y moves the cubes $L_z(\tilde{Q}_{\boldsymbol{v}(1)})$ in the y-direction to the center so that their y-coordinate becomes roughly 0. Then the mapping L_x moves the cubes $L_y\big(L_z(\tilde{Q}_{\boldsymbol{v}(1)})\big)$ in the x-direction to the center. In this way we map $\tilde{Q}_{\boldsymbol{v}(1)}$ into the tower formation.

Explicit construction of the mapping L. Let us now show in detail that we can do the construction, described above, by using bi-Lipschitz maps and that (6.1) will be satisfied at the end if we do this construction with a suitable way.

Let

$$t \in [-\tfrac{2}{3} + \tfrac{1}{100}, \tfrac{2}{3} - \tfrac{1}{100}] \text{ and } s \in [-\tfrac{7}{16} + \tfrac{1}{100}, \tfrac{7}{16} - \tfrac{1}{100}].$$

We define piecewise linear functions $h_t, g_t : [-1,1] \to [-1,1]$ such that $h_t(-1) = g_t(-1) = -1$, $h_t(1) = g_t(1) = 1$,

$$\begin{aligned}
h_s(x) &= x + s \text{ for } s > 0 \text{ and } \ x \in [-\tfrac{1}{2} - \tfrac{1}{16}, -\tfrac{1}{2} + \tfrac{1}{16}],\\
h_s(x) &= x + s \text{ for } s < 0 \text{ and } \ x \in [\tfrac{1}{2} - \tfrac{1}{16}, \tfrac{1}{2} + \tfrac{1}{16}],\\
g_t(x) &= x + t \text{ for } t > 0 \ \text{ and } \ x \in [-1 + \tfrac{1}{10}, 1 - \tfrac{2}{3}],\\
g_t(x) &= x + t \text{ for } t < 0 \ \text{ and } \ x \in [-1 + \tfrac{2}{3}, 1 - \tfrac{1}{10}],
\end{aligned}$$

and h_s, g_t are linear on the remaining intervals (see Fig. 12).

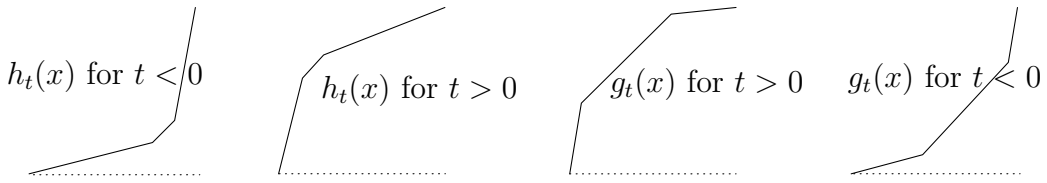

Fig. 12 Graphs of $h_t(x)$ and $g_t(x)$

It is easy to see that $h_s(x)$ and $g_t(x)$ are bi-Lipschitz functions. We would like to shift point $x = -\frac{1}{2}$ close to 0 with g_t, $t > 0$, and point $x = \frac{1}{2}$ close to 0 with g_t, $t < 0$. Moreover, by h_s, $s > 0$, we would like to shift point $x = -\frac{1}{2}$ to points with coordinates $\{-\frac{3}{8}, -\frac{1}{8}, \frac{5}{8}, \frac{7}{8}\}$ and by h_s, $s < 0$, point $x = \frac{1}{2}$ to points with coordinates $\{-\frac{7}{8}, -\frac{5}{8}, \frac{1}{8}, \frac{3}{8}\}$ (see (6.3) and Fig. 11).

Let

$$s_z, s_y, s_x : [-1,1]^2 \to [-\tfrac{2}{3} + \tfrac{1}{100}, \tfrac{2}{3} - \tfrac{1}{100}]$$

be fixed Lipschitz mappings such that

$$s_a(x,y) = 0 \text{ for every } (x,y) \in \partial[-1,1]^2 \text{ and } a \in \{x,y,z\}. \tag{6.4}$$

Let us define

$$\begin{aligned} L_z(x,y,z) &= (x,y,h_{s_z(x,y)}(z)),\\ L_y(x,y,z) &= (x,g_{s_y(x,z)}(y),z) \text{ and}\\ L_x(x,y,z) &= (g_{s_x(y,z)}(x),y,z). \end{aligned}$$

It is not difficult to see that these mappings are Lipschitz, they map $[-1,1]^3$ onto $[-1,1]^3$ and using (6.4) we obtain that they are identity on the boundary $\partial[-1,1]^3$. Moreover, the inverses are given by similar formula, e.g.

$$(L_z)^{-1}(x,y,z) = (x,y,h^{-1}_{s_z(x,y)}(z)),$$

and it is straightforward to verify that these maps are in fact bi-Lipschitz.

Let us denote by π_x, π_y and π_z projections to the corresponding coordinates, e.g. $\pi_x(x,y,z) = x$. By $\pi_{x,y}$, $\pi_{x,z}$, $\pi_{y,z}$ we denote the projection to corresponding planes, e.g. $\pi_{x,y}(x,y,z) = (x,y)$. Our aim is to construct mappings s_z, s_y, s_x such that the following is true.

First of all, L_z takes eight cubes $\tilde{Q}_{\boldsymbol{v}(1)}$ and shifts their z-coordinate to (6.3) as in Fig. 11. This can be clearly done using suitable Lipschitz mapping s_z which has constant value on each $\pi_{xy}(\tilde{Q}_{\boldsymbol{v}(1)})$. Then L_y takes cubes $L_z(\tilde{Q}_{\boldsymbol{v}(1)})$ and moves them in the y-direction so that it maps their centers (with y-coordinate $\frac{1}{2}$ or $-\frac{1}{2}$) to points with y-coordinate 0 , i.e.,

$$\text{for every } (x,z) \in \pi_{x,z}\big(L_z(\tilde{Q}_{\boldsymbol{v}(1)})\big) \text{ we have } s_y(x,z) = \pm\frac{1}{2}.$$

It is clear that we can select such a Lipschitz map s_y. In the end L_x takes cubes $L_y(L_z(\tilde{Q}_{\boldsymbol{v}(1)}))$ and moves them in the x-direction so that it maps their centers (with x-coordinate $\frac{1}{2}$ or $-\frac{1}{2}$) to points with x-coordinate 0, i.e.,

$$\text{for every } (y,z) \in \pi_{y,z}\big(L_y(L_z(\tilde{Q}_{\boldsymbol{v}(1)}))\big) \text{ we have } s_x(y,z) = \pm\frac{1}{2}.$$

Again we can choose such a lipschitz map s_x. At the end we have that centers of cubes $L(\tilde{Q}_{\boldsymbol{v}(1)})$ have both x and y coordinates 0 and hence they are in the tower formation.

It remains to show that (6.1) holds for carefully chosen s_z, s_y and s_x as above. We do not give the exact formulas for s_z, s_y and s_x as it would be lengthy and non-transparent. Instead we explain on a series of pictures that we can achieve that the images of red pipes from Fig. 10 do not intersect $\mathcal{S}_\theta$ from Fig. 9. Let us start with those red tubes that are "parallel" to x and y coordinates and connect $\tilde{Q}_{\boldsymbol{v}(1)}$ to $\partial[-1,1]^3$. By (6.2) the mapping L_p is just the identity on them. We draw projection to xy-plane of images of these tubes under each mapping L_z, L_y and then L_x.

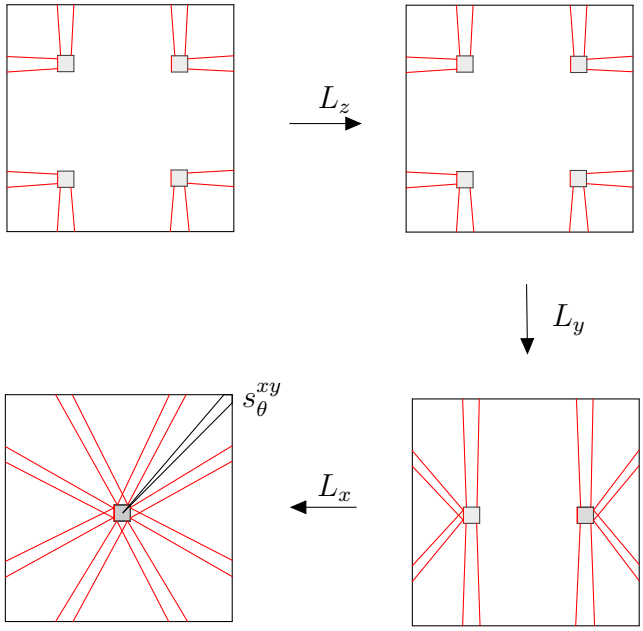

Fig. 13 L(red tubes parallel to x and y) does not intersect $\mathcal{S}_\theta$ (projection to xy-plane)

The definition of corners (see Fig. 5 and Fig. 8) and $\mathcal{S}_\theta$ (see Fig. 9) guarantees that the projection of red tubes ("parallel" to x and y coordinates) is really as in the last picture (bottom-left one) and hence it does not intersect $\mathcal{S}_\theta$ if θ is chosen sufficiently small (but fixed). Moreover, it is not difficult to see from these pictures that this can be done using Lipschitz functions s_z, s_y and s_x with the properties required above.

Now, let us consider red tubes that are "parallel" to x and y axis and connect $\tilde{Q}_{\boldsymbol{v}(1)}$ together. By (6.2) the mapping L_p is identity on them. Again we draw projections to xy-plane of images of these tubes under the mappings L_z, L_y and then L_x - see Fig. 14 below. The mapping L_z just maps $\tilde{Q}_{\boldsymbol{v}(1)}$ to different z coordinates but their xy-projection remains the same. Then L_y maps red tubes (originally parallel to y-axis) to some S shaped tubes (in the yz-projection) - the red object above and below black cubes on the bottom-right picture. Then L_x maps those S shapes left to the black cube on the bottom-left picture. The red tubes parallel to x are mapped below black cubes by L_y and then it remains below when we map by L_x. Again the image of red tubes does not intersect $\mathcal{S}_\theta$ and it is not difficult to see from these pictures that this can be done using Lipschitz functions s_z, s_y and s_x with the properties required above.

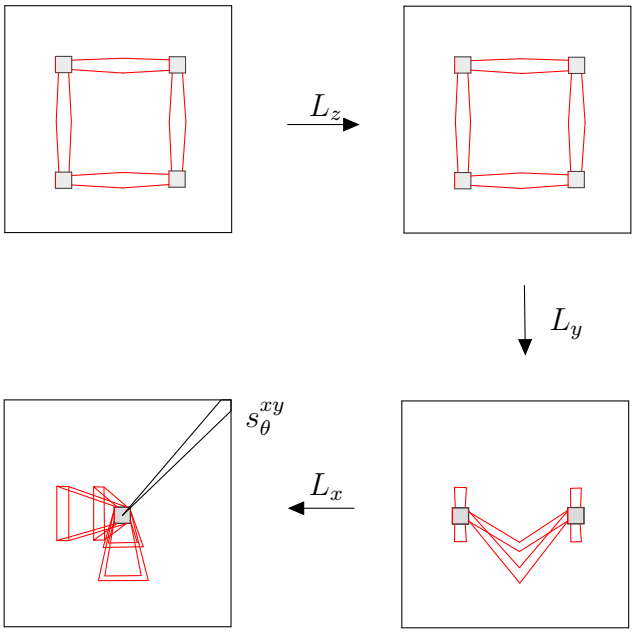

Fig. 14 L(red tubes parallel to x and y) does not intersect $\mathcal{S}_\theta$ (projection to xy-plane)

It remains to consider the image of red tubes that are "parallel" to z-axis. The situation is not as simple as the previous case here and we cannot simply use $L_x \circ L_y \circ L_z$ and we have to consider also the mapping L_p. There are two reasons for this. First of all, the red tubes intersect $\partial[-1,1]^3$ and $L_x \circ L_y \circ L_z$ is the identity on $\partial[-1,1]^3$. Thus we have two squares from $\pi_{x,y}(\tilde{Q}_{\boldsymbol{v}(1)}) \times \{-1,1\}$ that intersect $\mathcal{S}_\theta$ (those in the upper-left corner, i.e. for $\boldsymbol{v}(1) = (1,1,1)$) and we have to move these two squares away using the mapping L_p. Secondly, $L_x \circ L_y \circ L_z$ is just a translation on $\partial\tilde{Q}_{\boldsymbol{v}(1)}$ but the red tubes intersect $\partial\tilde{Q}_{\boldsymbol{v}(1)}$. On the two faces of $\partial\tilde{Q}_{\boldsymbol{v}(1)}$ parallel to xy-plane we have two big red squares (intersection of red pipes and $\partial\tilde{Q}_{\boldsymbol{v}(1)}$) that are moved by $L_x \circ L_y \circ L_z$ so that the center of the image becomes $(0,0)$ in the xy-plane. Therefore these squares clearly intersect $\mathcal{S}_\theta$. We correct this by applying L_p of the second generation (corresponding to the definition of L_2) and shift these red squares elsewhere.

Let us now explain how to define the mapping $L_p : [-1,1]^3 \to [-1,1]^3$. Recall that L_p is just an identity on a big part, see (6.2). Firstly, we define a mapping $\ell_p^t : [-1,1]^2 \to [-1,1]^2$ for $t \in (0,1]$ that shrinks the red square t-times and moves it outside of the first quadrant (see Fig. 15) for small values of t. More precisely, let $0 < a < 1$ be a fixed number such that the red square is $[-1+a, 1-a]^2$. We define

$$\ell_p^t(x) = tx - (1,1) + (t,t) \text{ for } x \in [-1+a, 1-a]^2.$$

It is clear that

$$\ell_p^t\big([-1+a, 1-a]^2\big) = [-1+ta, -1+2t-ta]^2$$

and hence it moves the red square outside of the first quadrant for $t = \frac{1}{2}$. Moreover, we define ℓ_p^t on $[-1,1]^2 \setminus [-1+a, 1-a]^2$ (similarly to (2.4)) so that the whole mapping is bi-Lipschitz (with constant $C\frac{1}{t}$) and it is identity on $\partial[-1,1]^2$.

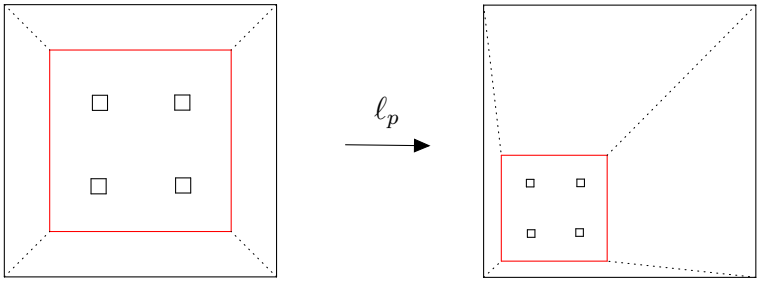

Fig. 15 Definition of the mapping ℓ_p^t

We define

$$L_p(x,y,z) = \begin{cases} (x,y,z), & \text{for } z \in [-1+\frac{1}{20}, 1-\frac{1}{20}], \\ \left(\ell_p^{-\frac{40}{3}z+\frac{41}{3}}(x,y), z\right), & \text{for } z \in [1-\frac{1}{20}, 1], \\ \left(\ell_p^{\frac{40}{3}z+\frac{41}{3}}(x,y), z\right), & \text{for } z \in [-1, -1+\frac{1}{20}]. \end{cases} \tag{6.5}$$

It is easy to see that this mapping is bi-Lipschitz and maps $[-1,1]^3$ onto $[-1,1]^3$. Moreover, it maps the red square on the planes $z=1$ and $z=-1$ outside of the first quadrant and it does similar thing for nearby values of z. Now, we can define

$$L_1 := L_x \circ L_y \circ L_z \circ L_p.$$

Let us now briefly explain how to define L_2 and glue things together. Then we show the key property (6.1) for red tubes parallel to z-axis. We know that $L_1(\tilde{Q}_{\boldsymbol{v}(1)})$ are cubes of side-length $2\tilde{r}_1$. Let us denote their centers as $s_{\boldsymbol{v}(1)}$, i.e.,

$$L_1(\tilde{Q}_{\boldsymbol{v}(1)}) = Q(s_{\boldsymbol{v}(1)}, \tilde{r}_1).$$

We define

$$L_z^2(x) = s_{\boldsymbol{v}(1)} + \tilde{r}_1 L_z\Big(\frac{1}{\tilde{r}_1}(x - s_{\boldsymbol{v}(1)})\Big) \text{ for } x \in Q(s_{\boldsymbol{v}(1)}, \tilde{r}_1).$$

It is easy to check that L_z^2 are bi-Lipschitz (with the same constant L_z) and they map $Q(s_{\boldsymbol{v}(1)}, \tilde{r}_1)$ onto $Q(s_{\boldsymbol{v}(1)}, \tilde{r}_1)$. In a similar spirit we define

$$L_p^2(x) = s_{\boldsymbol{v}(1)} + \tilde{r}_1 L_p\Big(\frac{1}{\tilde{r}_1}(x - s_{\boldsymbol{v}(1)})\Big) \text{ for } x \in Q(s_{\boldsymbol{v}(1)}, \tilde{r}_1) \tag{6.6}$$

but we would like to define it also on $Q(s_{\boldsymbol{v}(1)} + 2\tilde{r}_1\mathbf{e}_3, \tilde{r}_1)$ and $Q(s_{\boldsymbol{v}(1)} - 2\tilde{r}_1\mathbf{e}_3, \tilde{r}_1)$ (here $\mathbf{e}_3 = (0,0,1)$) so we connect it with the identity mapping outside of these three cubes. Formally we define (compare with (6.5))

$$L_p(x,y,z) = \begin{cases} \left(\ell_p^{\frac{1}{3}z}(x,y), z\right), & \text{for } (x,y,z) \in Q((0,0,2),1), \\ \left(\ell_p^{-\frac{1}{3}z}(x,y), z\right), & \text{for } (x,y,z) \in Q((0,0,-2),1), \end{cases}$$

and it is easy to see that L_p is now identity on $\partial\big([-1,1]^2 \times [-3,3]\big)$. The definition (6.6) now defines L_p^2 also on $Q(s_{\boldsymbol{v}(1)} + 2\tilde{r}_1\mathbf{e}_3, \tilde{r}_1)$ and $Q(s_{\boldsymbol{v}(1)} - 2\tilde{r}_1\mathbf{e}_3, \tilde{r}_1)$. It is not difficult to see that L_p^2 shifts the red squares on the z boundaries of $\partial Q(s_{\boldsymbol{v}(1)}, \tilde{r}_1)$ "outside of

the first quadrant" similarly as L_p does for $[-1,1]^3$. Similarly we define L_y^2 (resp. L_x^2) on the cubes $L_z^2(L_p^2(Q(s_{\boldsymbol{v}(1)},\tilde{r}_1)))$ (respectively on $L_y^2(L_z^2(L_p^2(Q(s_{\boldsymbol{v}(1)},\tilde{r}_1)))))$.

Finally, we show that (6.1) holds for red tubes from Fig. 10 parallel to z-axis for the mapping $L_p^2 \circ L_x \circ L_y \circ L_z \circ L_p$. Again we show a series of pictures for projections to xy-plane. The red squares correspond to intersection of red pipes with $\partial[-1,1]^2$ (respectively $\tilde{Q}_{\boldsymbol{v}(1)}$ on the last two pictures).

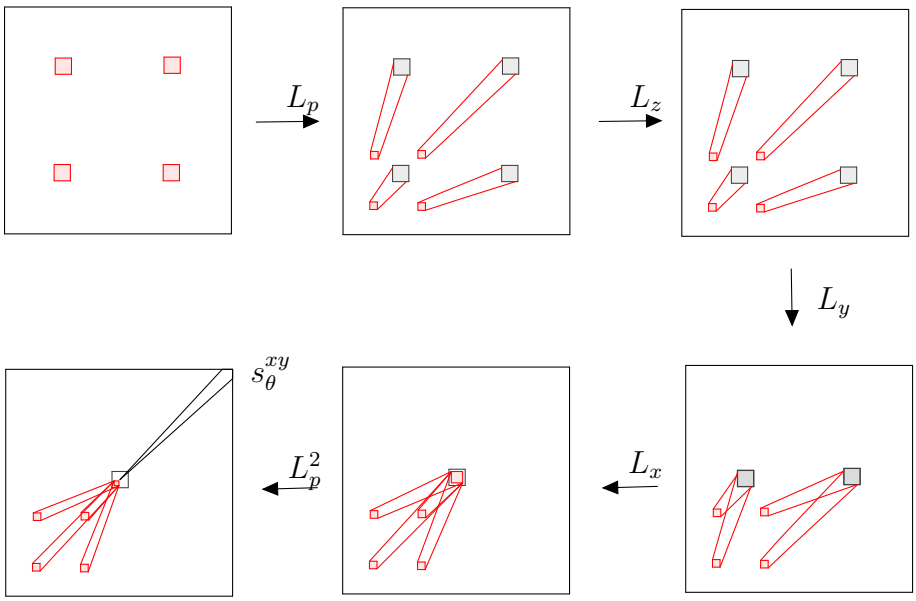

Fig. 16 L(red tubes parallel to z) does not intersect $\mathcal{S}_\theta$ (projection to xy-plane)

Our definition of $\mathcal{S}_\theta$ (see Fig. 9) guarantees that the projection of red tubes ("parallel" to z-coordinate) does not intersect $\mathcal{S}_\theta$. Again it is not difficult to see from these pictures that this can be done using Lipschitz functions s_z, s_y and s_x with the properties required above. This finishes the proof of (6.1) and also the construction of L_1.

7. Proof of Theorem 1.3

Proof of Theorem 1.3. Recall that the Cantor sets C_A and C_B are defined at the beginning of section 5 and that the set $\mathcal{S}_\theta$ is defined at the beginning of previous section. Suppose that:

(1) Mapping $g : \mathbb{R}^3 \to \mathbb{R}^3$ is the homeomorphism (defined in section 5) which maps the Cantor set C_A onto the Cantor set C_B and maps each set $Q'_{\boldsymbol{v}(k)} \setminus Q_{\boldsymbol{v}(k)}$ onto the corresponding set $\tilde{Q}'_{\boldsymbol{v}(k)} \setminus \tilde{Q}_{\boldsymbol{v}(k)}$ radially and maps corners to corners.
(2) Mapping $L : \mathbb{R}^3 \to \mathbb{R}^3$ is the bi-Lipschitz map (defined in section 6) which takes the Cantor set C_B onto the Cantor's tower C_B^T and for which the preimage $(L \circ g)^{-1}(\mathcal{S}_\theta)$ is contained in the union of the corners (see (6.1)).
(3) Let ω_θ be the mapping which is the identity on $\mathbb{R}^3 \setminus \mathcal{S}_\theta$ and winds $\mathcal{S}_\theta$ such that the angle θ is stretched onto angle $2\pi + \theta$ so that the glued mapping is continuous.

We need to wind ω_θ not radially but in supremum norm. Formally let $S : \mathbb{R}^3 \to \mathbb{R}^3$ be a bi-Lipschitz mapping which maps the unit cube $(-1,1)^3$ onto a cylinder $B^2(0,1)\times(-1,1)$ naturally (so that $S(\mathcal{S}_\theta)$ corresponds to angle $\varphi \in [\frac{\pi}{4}-\frac{\theta}{2}, \frac{\pi}{4}+\frac{\theta}{2}]$). Let (r,φ) be the polar coordinates of the point (x_1,x_2) and define $\tilde{\omega}_\theta : \mathbb{R}^3 \to \mathbb{R}^3$ as the winding map (the radial one)

$$\tilde{\omega}_\theta(x) = \begin{cases} \Big(r\cos\Big(a(\theta,\varphi)+\frac{\pi}{4}-\frac{\theta}{2}\Big), r\sin\Big(a(\theta,\varphi)+\frac{\pi}{4}-\frac{\theta}{2}\Big), x_3\Big), & \text{if } x \in \mathcal{S}_\theta \\ x, & \text{otherwise,} \end{cases}$$

where $a(\theta,\varphi) := \frac{\theta+2\pi}{\theta}(\varphi - \frac{\pi}{4} + \frac{\theta}{2})$. Then we set

$$\omega_\theta = S^{-1} \circ \tilde{\omega}_\theta \circ S.$$

Now we define the mapping $f : (-1,1)^3 \to (-1,1)^3$ by

$$f := g^{-1} \circ L^{-1} \circ \omega_\theta \circ L \circ g\,.$$

This composition maps C_A onto C_B, then C_B onto Cantor tower $C_B^T \subset (0,0)\times[-1,1]$, then winds twice around $(0,0)\times[-1,1]$ and then maps everything back to C_A. In this way $C_A \subset \mathcal{B}_f$ and $C_A \subset f(\mathcal{B}_f)$.

Step 1: First we need to show that f is absolutely continuous on almost every line parallel to coordinate axis. Because f is obviously a locally Lipschitz map outside the set C_A (as it is a composition of locally Lipschitz maps there) it suffices to show that f is absolutely continuous along those line segments I parallel to coordinate axes for which $I \cap C_A \neq \emptyset$. For this purpose, suppose that I_i is a line segment parallel to x_i-axis, such that $I_i \cap C_A \neq \emptyset$. We claim that actually

$$f(x) = x \quad \text{for all } x \in I_i.$$

To show this, we first recall the following definitions from section 6:

$$\mathbb{BAD} := \big\{x \in (-1,1)^3 : L(g(x)) \in \mathcal{S}_\theta\big\}$$

and

$$\begin{aligned}\mathbb{BAD}_k &:= \Big\{x \in \bigcup_{\boldsymbol{v}(k)\in\mathbb{V}^k} Q'_{\boldsymbol{v}(k)} \setminus Q_{\boldsymbol{v}(k)} : L(g(x)) \in \mathcal{S}_\theta\Big\} \\ &= \Big\{x \in \bigcup_{\boldsymbol{v}(k)\in\mathbb{V}^k} Q'_{\boldsymbol{v}(k)} \setminus Q_{\boldsymbol{v}(k)} : x \in \mathbb{BAD}\Big\}.\end{aligned}$$

It follows from (6.1) in the construction of the bi-Lipschitz map L that

$$\mathbb{BAD}_k \subset \bigcup_{\boldsymbol{v}(k)\in\mathbb{V}^k} C_{\boldsymbol{v}(k)},$$

and hence using (5.18) we have

$$\mathcal{L}^3(\mathbb{BAD}_k) \lesssim 2^{-2k}. \tag{7.1}$$

On the other hand, it follows from the definition of sets $C_{\boldsymbol{v}(k)}$ that $I_i \cap C_{\boldsymbol{v}(k)} = \emptyset$ for every $\boldsymbol{v}(k)$ (since $I_i \cap C_A \neq \emptyset$) which implies

$$I_i \cap \mathbb{BAD} = \emptyset.$$

Thus, for every $x \in I_i$ we have

$$\begin{aligned} f(x) &= (g^{-1} \circ L^{-1} \circ \omega_\theta \circ L \circ g)(x) \\ &= (g^{-1} \circ L^{-1} \circ \mathrm{id} \circ L \circ g)(x) = x, \end{aligned} \tag{7.2}$$

and the claim follows.

Step 2: Next we will show that

$$\int_{(-1,1)^3} |Df(x)|^2 \log^\alpha(e + |Df(x)|)\,\mathrm{d}x < \infty$$

for every $\alpha < -1$. For this purpose we observe first that $\omega_\theta(x) = x$ for $x \in (0,0) \times [-1,1]$, and that $L(g(C_A)) \subset (0,0) \times [-1,1]$. Then, as in (7.2), we obtain $f = \mathrm{id}$ on C_A. Therefore

$$|Df(x)| = 1 \quad \text{for almost every } x \in C_A.$$

Thus, it suffices to estimate $|Df(x)|$ on $(-1,1)^3 \setminus C_A$. For this purpose, we point out that

(i) g is a locally bi-Lipschitz map on $(-1,1)^3 \setminus C_A$ and
$$g((-1,1)^3 \setminus C_A) = (-1,1)^3 \setminus C_B.$$
(ii) $h := L^{-1} \circ \omega_\theta \circ L$ is a Lipschitz map on $(-1,1)^3 \setminus C_B$ and
$$h((-1,1)^3 \setminus C_B) = (-1,1)^3 \setminus C_B$$
and h satisfies the Lusin (N^{-1}) condition.
(iii) g^{-1} is a locally Lipschitz map on $(-1,1)^3 \setminus C_B$.

Analogously to the reasoning in the paragraph before (4.7) we obtain from (i)–(iii) that the chain rule applies to the mapping $f = g^{-1} \circ h \circ g$ almost everywhere outside the set C_A, and therefore

$$\begin{aligned} |Df(x)| &\le |Dg^{-1}(h(g(x)))| \cdot |Dh(g(x))| \cdot |Dg(x)| \\ &\le \mathrm{Lip}(h)\, |Dg^{-1}(h(g(x)))| \cdot |Dg(x)| \end{aligned} \tag{7.3}$$

for almost every $x \in (-1,1)^3 \setminus C_A$. Next we recall that $f = \mathrm{id}$ outside the set $\mathbb{BAD}$ (see (7.2)) and therefore it suffices to show that

$$\int_{\mathbb{BAD}} |Df|^2 \log^\alpha(e + |Df|) = \sum_{k=1}^{\infty} \int_{\mathbb{BAD}_k} |Df|^2 \log^\alpha(e + |Df|) < \infty$$

for every $\alpha < -1$. By (5.13) we have

$$|Dg(x)| \sim 2^{k - \beta k}, \tag{7.4}$$

for almost every every $x \in \mathbb{BAD}_k$. Moreover, we also have

$$(h \circ g)\big(Q'_{\boldsymbol{v}(k)} \setminus Q_{\boldsymbol{v}(k)}\big) = \tilde{Q}'_{\boldsymbol{v}(k)} \setminus \tilde{Q}_{\boldsymbol{v}(k)},$$

and thus by (5.15)

$$|Dg^{-1}(g(h(x)))| \lesssim 2^{k\beta}, \tag{7.5}$$

for almost every $x \in \mathbb{BAD}_k$. If we now combine (7.1), (7.3), (7.4) and (7.5) we get

$$\sum_{k=1}^{\infty} \int_{\mathbb{BAD}_k} |Df|^2 \log^{\alpha}(e + |Df|) \sim \sum_{k=0}^{\infty} 2^{-2k} 2^{2k} \log^{\alpha}(e + 2^k) \sim \sum_{k=1}^{\infty} k^{\alpha} < \infty$$

for every $\alpha < -1$, and the claim follows. This is already enough to prove Theorem 1.3. However, it is interesting to know what level of integrability we may obtain for the distortion functions $K_O(\cdot, f)$ and $K_I(\cdot, f)$ in the construction. Therefore, we will add one additional step in the proof to estimate the distortions as well.

Step 3: Recall again that $f = \mathrm{id}$ on $(-1,1)^3 \setminus \mathbb{BAD}$ and therefore

$$K_I(x, f) = 1 \quad \text{for almost every } x \in (-1,1)^3 \setminus \mathbb{BAD}, \text{ and}$$
$$K_O(x, f) = 1 \quad \text{for almost every } x \in (-1,1)^3 \setminus \mathbb{BAD}.$$

As before we can apply the chain rule a.e. outside of C_A and we get

$$\begin{aligned} K_O(x, f) = \frac{|Df(x)|^n}{J_f(x)} &\leq \frac{|Dg^{-1}(h(g(x)))|^n \operatorname{Lip}^n(h) |Dg(x)|^n}{J_{g^{-1}}(h(g(x))) J_h(g(x)) J_g(x)} \\ &\leq C K_O(h(g(x)), g^{-1}) K_O(x, g). \end{aligned}$$

Analogously we obtain for adjugate matrices $|\operatorname{adj}(AB)| \leq \operatorname{adj}(A) \operatorname{adj}(B)$ and hence

$$K_I(x, f) \leq C K_I(h(g(x)), g^{-1}) K_I(x, g).$$

From the estimates (5.14) and (5.16) in section 5.2 and from the fact $\mathbb{BAD}_k \subset G_k \cup E_k$ (see (6.1)) it follows that

$$K_I(x, f) \leq C 2^{4k} \quad \text{and} \quad K_O(x, f) \leq C 2^{3k}$$

for almost every $x \in \mathbb{BAD}_k$. Using this and (5.18) we get

$$\begin{aligned} \int_{(-1,1)^3} K_I(x, f)^p \, \mathrm{d}x &= \int_{(-1,1)^3 \setminus \mathbb{BAD}} K_I(x, f)^p \, \mathrm{d}x + \sum_{k=1}^{\infty} \int_{\mathbb{BAD}_k} K_I(x, f)^p \, \mathrm{d}x \\ &\leq 2^3 + \sum_{k=1}^{\infty} 2^{-2k} 2^{4kp} < \infty \end{aligned}$$

for every $p < \frac{1}{2}$. Similarly, we get

$$\begin{aligned} \int_{(-1,1)^3} K_O(x, f)^q \, \mathrm{d}x &= \int_{(-1,1)^3 \setminus \mathbb{BAD}} K_O(x, f)^q \, \mathrm{d}x + \sum_{k=1}^{\infty} \int_{\mathbb{BAD}_k} K_O(x, f)^q \, \mathrm{d}x \\ &\leq 2^3 + \sum_{k=1}^{\infty} 2^{-2k} 2^{3kq} < \infty \end{aligned}$$

for every $q < \frac{2}{3}$. □

Remark 7.1. As it was pointed out in the introduction, we do not know what happens for the size of the branch set of continuous, discrete an open mappings with positive Jacobian almost everywhere in the borderline space $W^{1,n-1}$. However, it is possible to slightly improve the integrability of the distortions in Theorem 1.3 by modifying the construction of the mapping f in the proof:

Proposition 7.2. *Denote $Q_0 := (-1,1)^3$, and suppose that*

$$0 < q < 2/3 \quad \text{and} \quad 0 < r < 2/3.$$

Then there exists a continuous, discrete and open mapping of finite distortion $f \in W^{1,p}(Q_0, Q_0)$, for all $p \in [1,2)$, with

$$K_I(\cdot, f) \in L^q(Q_0) \quad \text{and} \quad K_O(\cdot, f) \in L^r(Q_0)$$

such that $J_f > 0$ almost everywhere and

$$\mathcal{L}^3(\mathcal{B}_f) > 0 \quad \text{and} \quad \mathcal{L}^3(f(\mathcal{B}_f)) > 0.$$

We will only sketch the proof of the proposition above and highlight the differences to the construction in Theorem 1.3:

Sketch of the proof of Proposition 7.2. Instead of considering only two Cantor sets we will work now with three different Cantor sets

$$C_A := C[\{a_k\}_{k=1}^{\infty}], \quad C_B := C[\{b_k\}_{k=1}^{\infty}] \quad \text{and} \quad C_C := C[\{c_k\}_{k=1}^{\infty}]$$

defined by the sequences

$$a_k = \frac{1}{2}\Big(1 + \frac{1}{2^k}\Big), \quad b_k = 2^{-\beta k} \quad \text{and} \quad c_k = \frac{1}{2}\Big(1 + \frac{1}{2^{k\gamma}}\Big),$$

where $\beta > 0$ can be chosen with a similar way as in the proof of Theorem 1.3, and the exponent $0 < \gamma < 1$ is defined later. In addition, suppose that the mappings g, L, and ω_θ are defined similarly as in the proof of Theorem 1.3. We also consider a new homeomorphism $h : (-1,1)^3 \to (-1,1)^3$ which maps the Cantor set C_C onto C_B. The mapping h can be defined with a similar fashion as the homeomorphism g in section 5. Then we set

$$f := h^{-1} \circ L^{-1} \circ \omega_\theta \circ L \circ g.$$

One may check that this will give us a Sobolev mapping with positive Jacobian almost everywhere. Moreover, by calculating similarly as in the proof of Theorem 1.3 we get the following estimates:

(1) First we estimate the Sobolev norm in the set $\mathbb{BAD}$ simply by applying the chain rule similarly as in the proof of Theorem 1.3. This gives us the following estimate:

$$\int_{\mathbb{BAD}} |Df(x)|^p \, \mathrm{d}x \lesssim \sum_{k=1}^{\infty} 2^{-2k}(2^k \cdot 1)^p.$$

The sum above converges for all $0 < p < 2$.

(2) To estimate the Sobolev norm of the mapping outside the set $\mathbb{BAD}$ we observe by analyzing the map

$$f = h^{-1} \circ \mathrm{id} \circ g$$

in each of the sets S_k more carefully (for the definition of the set S_k, see section 5) that

$$Df(x) \sim \begin{pmatrix} 1 & 0 & 0 \\ 0 & 1 & 0 \\ 0 & 0 & 2^{\alpha k} 2^{-\gamma k} \end{pmatrix} \quad \text{for every } x \in S_k$$

up to some permutation of the column vectors. This will give us the following estimate:

$$\int_{(-1,1)^3\setminus\mathbb{BAD}} |Df(x)|^p \,\mathrm{d}x \lesssim \sum_{k=1}^{\infty} 2^{-k}(2^k 2^{-\gamma k})^p.$$

The sum above converges whenever $\gamma > \frac{p-1}{p}$.

(3) We estimate the integral of K_I^q in the set $\mathbb{BAD}$ by applying the chain rule, which gives us:

$$\int_{\mathbb{BAD}} K_I(x,f)^q \,\mathrm{d}x \lesssim \sum_{k=1}^{\infty} 2^{-2k}(2^{2k}2^{2\gamma k})^q.$$

This sum converges whenever $0 < \gamma < \frac{1-q}{q}$.

(4) Next, by applying the representation for the matrix $Df(x)$ in (2) we may estimate the integral of K_I^q in the set $(-1,1)^3 \setminus \mathbb{BAD}$ as follows:

$$\int_{(-1,1)^3\setminus\mathbb{BAD}} K_I(x,f)^q \,\mathrm{d}x \lesssim \sum_{k=1}^{\infty} 2^{-k}(2^{2k}2^{-2\gamma k})^q.$$

This sum converges whenever $\gamma > \frac{2q-1}{2q}$.

(5) We estimate the integral of K_O^r in the set $\mathbb{BAD}$ by simply applying the chain rule. This gives us the following estimate:

$$\int_{\mathbb{BAD}} K_O(x,f)^r \,\mathrm{d}x \lesssim \sum_{k=1}^{\infty} 2^{-2k}(2^{2k}2^{2\gamma k})^r.$$

This sum converges whenever $0 < \gamma < \frac{1-r}{r}$.

(6) Again, by applying the representation of $Df(x)$ in (2), we may estimate the integral of K_O^r in the set $(-1,1)^3 \setminus \mathbb{BAD}$ as follows:

$$\int_{(-1,1)^3\setminus\mathbb{BAD}} K_O(x,f)^r \,\mathrm{d}x \lesssim \sum_{k=1}^{\infty} 2^{-k}(2^{k}2^{-\gamma k})^r.$$

This sum converges whenever $\gamma > \frac{r-1}{r}$.

Suppose now that the parameters $1 \le p < 2$, $0 < q < 2/3$ and $0 < r < 2/3$ are fixed. Then we may choose the parameter γ such a way that it satisfies the following condition

$$\max\Big\{\frac{p-1}{p}, \frac{r-1}{r}, \frac{2q-1}{2q}\Big\} < \gamma < \min\Big\{\frac{1-r}{r}, \frac{1-q}{q}\Big\}.$$

More precisely, it is enough to choose γ such that

$$\frac{1}{2} < \gamma < \frac{1}{2} + \varepsilon,$$

where $\varepsilon > 0$ is some sufficiently small number depending only on the values of the parameters q and r. With such a parameter γ we may see that the mapping f satisfies all the estimates (1)–(6) above. Other parts of the proof we leave for the reader.

□

Acknowledgments
The authors want to express their gratitudes to Kai Rajala, Aapo Kauranen and Pawel Goldstein for their valuable comments.

References

1. M. Aaltonen, Monodromy representations of completed coverings, Rev. Mat. Iberoam. **32** (2016), no. 2, 533–570.
2. M. Aaltonen and P. Pankka, Local monodromy of branched covers and dimension of the branch set, Preprint.
3. L. Ambrosio, N. Fusco and D. Pallara, Functions of bounded variation and free discontinuity problems, Oxford Mathematical Monographs, The Clarendon Press, Oxford University Press, New York, 2000.
4. K. Astala, T. Iwaniec and G. Martin, Elliptic partial differential equations and quasiconformal mappings in the plane, Princeton University Press, Princeton, NJ, 2009.
5. J. Ball, Global invertibility of Sobolev functions and the interpenetration of matter, Proc. Roy. Soc. Edinburgh Sect. A **88** (1981), 315–328.
6. C.J. Bishop, Quasiconformal mappings which increase dimension, Acad. Sci. Fenn. Ser. A I Math. **24** (1999), 397–407.
7. A.V. Chernavskiĭ, Finite-to-one open mappings of manifolds (Russian), Mat. Sb. **65** (1964), 357–369.
8. A.V. Chernavskiĭ, Remarks on the paper "On finite-to-one open mappings of manifolds" (Russian), Mat. Sb. **66** (1965), 471–472.
9. M. Csörnyei, S. Hencl and J. Malý, Homeomorphisms in the Sobolev space $W^{1,n-1}$, J. Reine Angew. Math. **644** (2010), 221–235.
10. F.W. Gehring and J. Väisälä, The coefficients of quasiconformality of domains in space, Acta Math. **114** (1965), 1–70.
11. C.-Y. Guo, Mappings of finite distortion: global homeomorphism theorem, J. Geom. Anal. **25** (2015), 1969–1991.
12. J. Heinonen and P. Koskela, Sobolev mappings with integrable dilatations, Arch. Rational. Mech. Anal. **125** (1993), 81–97.
13. J. Heinonen and S. Rickman, Geometric branched covers between generalized manifolds, Duke Math. J., **113** (2002), no. 3, 465–529.
14. J. Heinonen and S. Rickman, Quasiregular maps $\mathbf{S}^3 \to \mathbf{S}^3$ with wild branch sets, Topology, **37** (1998), no. 1, 1–24.
15. S. Hencl and P. Koskela, Lectures on mappings of finite distortion, Lecture Notes in Mathematics, Vol. 2096, 2014, XI, 176 p.
16. S. Hencl and K. Rajala, Optimal assumptions for discreteness, Arch. Ration. Mech. Anal **207** (2013), 775–783.
17. S. Hencl and V. Tengvall, Sharpness of the the differentiability almost everywhere and capacitary estimates for Sobolev mappings, Rev. Mat. Iberoam. **33** (2017), no. 2, 595–622.
18. T. Iwaniec and G. Martin, Geometric function theory and non-linear analysis, Oxford Mathematical Monographs. The Clarendon Press, Oxford University Press, New York, 2001.
19. T. Iwaniec and V. Šverák, On mappings with integrable dilatation, Proc. Amer. Math. Soc. **118** (1993), 181–188.
20. J. Kauhanen, P. Koskela and J. Malý, Mappings of finite distortion: discreteness and openness, Arch. Ration. Mech. Anal. **160** (2001), no. 2, 135–151.
21. J. Kauhanen, P. Koskela, J. Malý , J. Onninen, X. Zhong: Mappings of finite distortion: Sharp Orlicz-conditions, Rev. Mat. Iberoam. **19** (2003), 857–872.
22. P. Koskela and J. Malý, Mappings of finite distortion: the zero set of the Jacobian, J. Eur. Math. Soc. (JEMS) **5** (2003), no. 2, 95–105.
23. P. Koskela and J. Onninen, Mappings of finite distortion: capacity and modulus inequalities, J. Reine Angew. Math. **599** (2006), 1–26.

24. O. Martio, A capacity inequality for quasiregular mappings, Ann. Acad. Sci. Fenn. Ser. A I Math. **474** (1970), 1–18.
25. O. Martio, S. Rickman and J. Väisälä, Deffinitions for quasiregular mappings, Ann. Acad. Sci. Fenn. Ser. A I Math. **448** (1969), 1–40.
26. J. Onninen, Differentiability of monotone Sobolev functions, Real Anal. Exch. **26** (2000), no. 2, 761–772.
27. E. A. Poletskiĭ, The modulus method for non-homeomorphic quasiregular mappings (Russian), Mat. Sb. **83** (1970), 261–273.
28. Y. G. Reshetnyak, Space mappings with bounded distortion, Translations of Mathematical Monographs, 73. American Mathematical Society, Providence, RI, 1989.
29. S. Rickman, Quasiregular mappings. Ergebnisse der Mathematik und ihrer Grenzgebiete (3) [Results in Mathematics and Related Areas (3)], 26. Springer-Verlag, Berlin, 1993.
30. V. Šverák, Regularity properties of deformations with finite energy, Arch. Rational Mech. Anal. **100** (1988), 105–127.
31. V. Tengvall, Differentiability in the Sobolev space $W^{1,n-1}$, Calc. Var. Partial Differential Equations **51** (2014), no. 1–2, 381–399.
32. J. Väisälä, Discrete open mappings on manifolds, Ann. Acad. Sci. Fenn. Ser. A I Math. **392** (1966), 1–10.
33. J. Väisälä, Modulus and capacity inequalities for quasiregular mappings, Ann. Acad. Sci. Fenn. Ser. A I Math. **509** (1972), 1–14.
34. J. Väisälä, Two new characterizations for quasiconformality, Ann. Acad. Sci. Fenn. Ser. A I **362** (1965), 1–12.

(Chang-Yu Guo) Department of Mathematics, University of Fribourg, Fribourg, Switzerland
E-mail address: changyu.guo@unifr.ch

(Stanislav Hencl) Department of Mathematical Analysis, Charles University, Sokolovská 83, 186 00 Prague 8, Czech Republic
E-mail address: hencl@karlin.mff.cuni.cz

(Ville Tengvall) Department of Mathematics and Statistics, University of Jyväskylä, P.O. Box 35, FI-40014 Jyväskylä, Finland
E-mail address: ville.tengvall@jyu.fi